Viscoelastic Characterization of Collagen-GAG Scaffolds

by

Matthew Q. Wong

SUBMITTED TO THE DEPARTMENT OF MECHANICAL ENGINEERING
IN PARTIAL FULFILLMENT OF THE REQUIREMENTS FOR THE DEGREE OF

BACHELOR OF SCIENCE IN AS RECOMMENDED BY THE DEPARTMENT OF MECHANICAL ENGINEERING
AT THE
MASSACHUSETTS INSTITUTE OF TECHNOLOGY

June 2006

Signature of Author: _____
Department of Mechanical Engineering
May 12, 2006

Certified by: _____
Lorna Gibson
Matoula S. Salapatas Professor of Material Science & Engineering
Thesis Supervisor

Accepted by: _____
John H. Lienhard V
Professor of Mechanical Engineering
Chairman, Undergraduate Thesis Committee

Viscoelastic Characterization of Collagen-GAG Scaffolds

by

Matthew Q. Wong

Submitted to the Department of Mechanical Engineering
on May 12, 2006 in Partial Fulfillment of the
Requirements for the Degree of Bachelor of Science as
Recommended by the Department of Mechanical Engineering

ABSTRACT

An experimental study was performed to determine whether or not collagen-GAG scaffolds exhibit linear viscoelastic behavior. Tension tests were performed on dry and hydrated engineered collagen-GAG scaffolds in order to develop a stress-strain curve. Strains that fell in the linear elastic region of these curves were selected and then used in stress relaxation tests that were also performed on dry and hydrated specimens. The relaxation modulus was calculated from the resulting stress relaxation curves at different strain levels and compared to each other to determine viscoelastic linearity. In addition to the determination of viscoelastic linearity, a water bath was designed in the hopes of performing stress relaxation tests in hydrated environment with the temperature maintained at 37°C, the temperature of the human body.

These tests will aid in the future studies of how cells contract and apply force to the scaffolds since no previous studies have looked at the time dependent mechanical properties of these scaffolds. Moreover, the data can be used in the future to determine whether the viscoelastic response contributes to cellular processes such as migration speeds, attachment, and contraction.

Thesis Supervisor: Lorna Gibson

Title: Matoulas Matoula S. Salapatas Professor of Material Science & Engineering

Table of Contents

Table of Figures

1. Introduction

Regenerative medicine is an emerging field in which specialists are trying to engineer products and techniques to regenerate tissue. Regenerative medicine offers several advantages over current standards which can often involve grafting, multiple surgeries, loss of tissue, scarring, and complex biocompatibility issues. The ability to regenerate tissue means that doctors no longer need to worry about the supply of tissue and the morbidity of donor sites involved in grafting. Also, regeneration minimizes the amount of scarring and tissue loss, which can cause not only physical limitations but can also be cosmetically disfiguring.

One example of a regenerative device is the collagen-glycosaminoglycan (GAG) scaffold which has been used to successfully regenerate skin (Yannas 1989). Despite its current success in this area, however, knowledge of the rheology of collagen-GAG scaffolds is necessary to understand how cells interact mechanically with the scaffold. The implantation of collagen-GAG scaffolds in a skin wound site can prevent wound contraction, which is associated with the formation of scar tissue (Yannas 2001). Since much of the interaction between the cells and the scaffold involves the contraction of the collagen-GAG matrix by the cells (Roy et al. 1997), mechanical characterization of these scaffolds is needed to achieve the maximum possible success in medical applications. In particular, because cells can interact with scaffolds over a period of several hours (Freyman et al. 2001), knowing this viscoelastic character of collagen-GAG scaffolds will provide important information that could be useful in developing a more concrete theory of how these scaffolds induce regeneration in skin and how they can be used to induce regeneration in other tissues.

This thesis will investigate the stress relaxation properties of collagen-GAG scaffolds in order to begin development of a viscoelastic model for these scaffolds. As there is currently very little known about the viscoelastic behavior of these scaffolds, the goal of this research is simply to obtain a stress relaxation profile of these scaffolds at different strain levels and to determine whether the scaffolds exhibit linear viscoelastic behavior or not. Additionally, because in practice, the scaffolds are in a hydrated environment that is at body temperature, it would be advantageous to examine these properties in hydrated specimens at 37°C. To achieve this purpose, I will also design a water bath that will be able to regulate the temperature of the liquid surrounding the specimen in its testing apparatus in order to perform tests under conditions that are more comparable to those of the human body.

2. Background

The current primary application of collagen-GAG scaffolds is in the regeneration of partial skin, and has been marketed as a commercial product by the company Integra®. Generally, in an adult, a full skin wound heals by contraction and the formation of stiff and fibrous scar tissue. The implantation of a collagen-GAG scaffold inhibits wound contraction and the resulting scar formation, allowing regeneration to occur (Yannas 2001).

Because the interaction of the cells and a collagen-GAG scaffold at a wound site is primarily mechanical, knowledge of how the mechanical properties of the scaffold affect the behavior of cells is important in developing a theoretical model for tissue regeneration that can be used to develop methods of regenerating tissues other than skin. Some research has been done to study how cells interact with a collagen-GAG matrix (Freyman et al. 2001) as well as some of the effects the mechanical properties of the scaffold on these cells (Roy et al. 1997).

This thesis focuses on building upon some of the existing mechanical research on collagen-GAG scaffolds (Harley et. al. 2004) in order to begin developing a viscoelastic model. One fundamental step in building such a model is to determine whether the material exhibits linear or nonlinear viscoelastic behavior (Yannas 1974). This thesis will apply knowledge of classical solid mechanics and use mechanical tests to determine whether these collagen-GAG scaffolds exhibit such linear viscoelasticity.

2.1 Contractile Theory of Wound Healing & Scar Formation

The contractile theory of wound healing and the consequent formation of scar tissue attempts to explain the response of tissue injury in adult mammals. In the first and second trimesters in a mother's womb, the mammalian fetus undergoes regenerative healing where damaged tissue will be completely regenerated by the body. In contrast, after the first two trimesters, the body begins to heal in a completely different manner. Wound healing in adult mammals is characterized by contraction of the wound and the subsequent formation of scar tissue at the wound site (Yannas 2001). This scar tissue often inhibits movement and is of course unsightly. Figure 2.1 shows an example of scar tissue formation and contraction in a patient who lost skin due to severe burns.

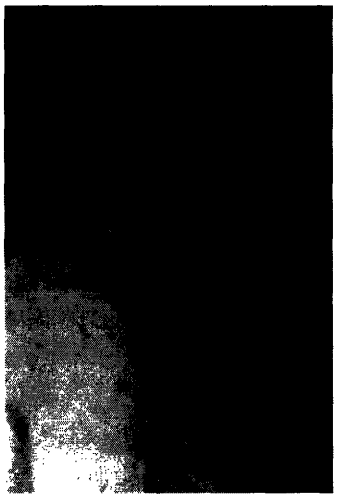

Figure 2.1: Scar tissue formation and contraction of a skin wound in a severe burn patient (Yannas 2001)

The two processes that comprise the adult mammalian response to injury are contraction and scar tissue formation. Figure 2.2 illustrates the progression of skin wound contraction in the guinea pig and the pig a period of several days.

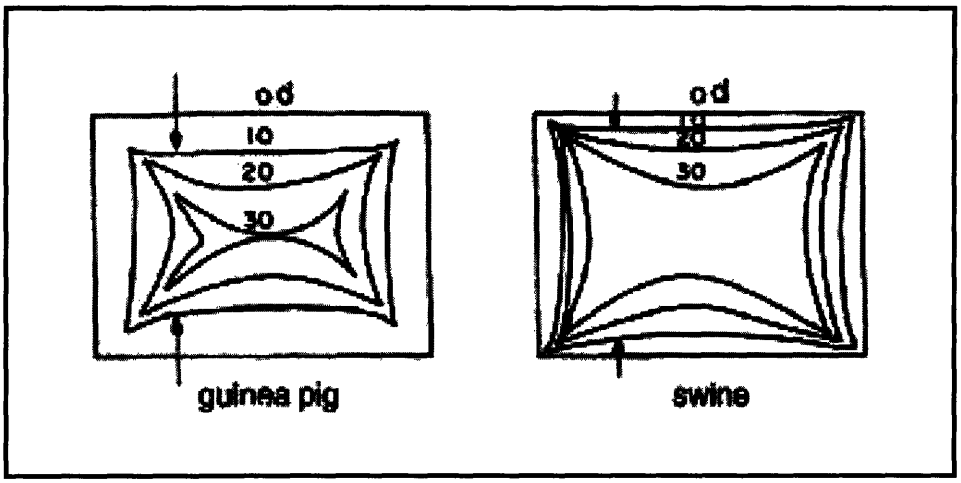

Figure 2.2: Wound contraction in the guinea pig and the swine (Yannas 2001)

In this case, the wound begins as a square and contracts along the edges of the wound to form a star shape that is typical of most scars in rodents. The amount of visible contraction depends on the amount of attachment between the skin and the underlying tissue. The skin of a rodent is much less attached to the underlying muscle tissue than in a human or a pig and thus, the area of the wound that closes is much greater in the rodent.

This mechanical closure of wounds by contraction induces and is closely associated with scar tissue formation. The complete biochemical pathways that bring about the formation of scar tissue are not readily known, but empirical studies have led to the development of the wound closure rule, which states that the initial wound area will completely be filled by some combination of contraction, scar tissue, and regenerated tissue. In adult mammals, no regeneration occurs, and thus, wounds naturally heal through contraction and scar tissue formation alone (Yannas 2001).

2.2 Cellular Mechanics of Wound Contraction

The contraction of a wound is the ultimate result of the contraction of many cells called fibroblasts that migrate into a wound site. Generally, fibroblasts are responsible for the creation of fibrous tissue such as the connective tissue found in dermis and in the extracellular matrix. When there is a wound in a vascularized tissue, the interaction of platelets in the blood with collagen initiate biochemical pathways that cause the formation of coagulation fibers and fibrin clots. These clots provide matrices that enable fibroblasts to migrate and settle inside the wound site. Once there, certain growth factors induce the fibroblasts to differentiate into myofibroblasts, which are the cells that ultimately provide the contractile force necessary to cause wound closure (Grinnell 1994).

These myofibroblasts provide force by attaching to struts in the network of fibers at a wound site and elongating (Freyman et al. 2001) and thereby bending or collapsing the struts that the cell has attached to. These cells can provide forces of up to approximately 3 nN of force and can take between two to four hours to reach their final morphological state (Freyman et al. 2002). In a typical skin wound, the myofibroblasts also tend to align along an axis and contract which allows the forces to sum together and results in contraction on the macroscopic level. This alignment of cells and the resulting contraction is also theorized to be what causes the alignment of fibers in scar tissue (Yannas 2001).

2.3 Contraction Blocking Theory of Regeneration

By the wound closure rule, preventing contraction and the associated scar tissue formation should result in the regeneration of tissue. Collagen-GAG scaffolds achieve this blocking of contraction by reducing the differentiation of fibroblasts into contractile myofibroblasts and by disorienting them to prevent the presence of a macroscopic contractile force.

2.3.1 Tissue Triad

Every organ in the body contains three types of tissues: epithelial tissue, basement membrane, and stroma or connective tissue. These three tissues are commonly referred to as the "tissue triad" (Yannas 2001). Of these tissues, the epithelial layer and basement membrane can regenerate spontaneously if damaged or removed, while the stroma, which is mainly composed of connective tissue, cannot. In the skin, for example, the epithelial tissue is the epidermis, the basement membrane is the epidermis-dermis interface, and the stroma is the dermis (Figure 2.3). The delineation of these three tissues is important to understanding the natural wound healing process.

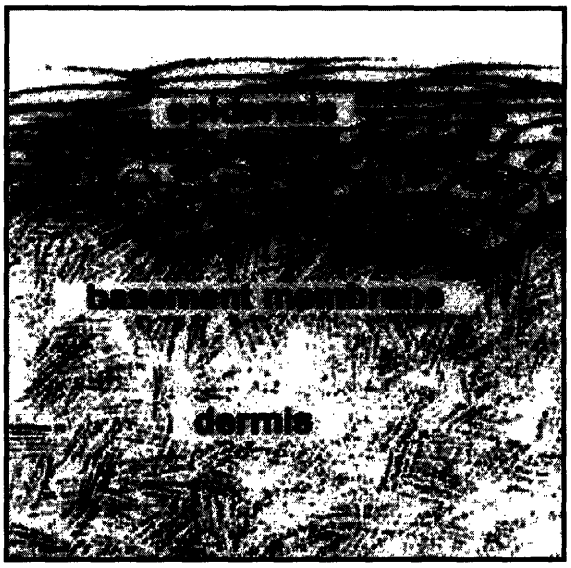

Figure 2.3: Tissue triad in skin (Yannas 2001)

2.3.2 Blocking Contraction

Although the epithelial tissue layer and basement membrane regenerate spontaneously, they will not form without the presence of the underlying stroma. Thus, the regeneration of an organ depends on the ability to regenerate the stroma, which in the case of the skin, is the dermis. According to the closure rule, the first step in this process is to prevent contraction and thereby prevent scar tissue formation.

Collagen-GAG scaffolds effectively prevent contraction at a wound site by reducing the number of myofibroblasts and by disrupting their organization in the wound site. Because of the manner in which the scaffold is prepared, the collagen banding is abolished and the scaffold does not aggregate platelets which induce the release of a growth factor called TGF-β. This growth factor contributes to the biochemical pathway that causes fibroblasts to differentiate into contractile myofibroblasts. Moreover, the scaffold binds extensively to myofibroblasts, which causes them to lose their orientation and disrupts the cohesion of the cell population. Because of this disorientation, the cells no longer contract along a common plane, and the sum of the vectorial forces is greatly reduced in magnitude (Yannas 1989). Figure 2.4 provides images of wound sites in which no scaffold has been inserted (top) and into which a scaffold has been inserted (bottom).

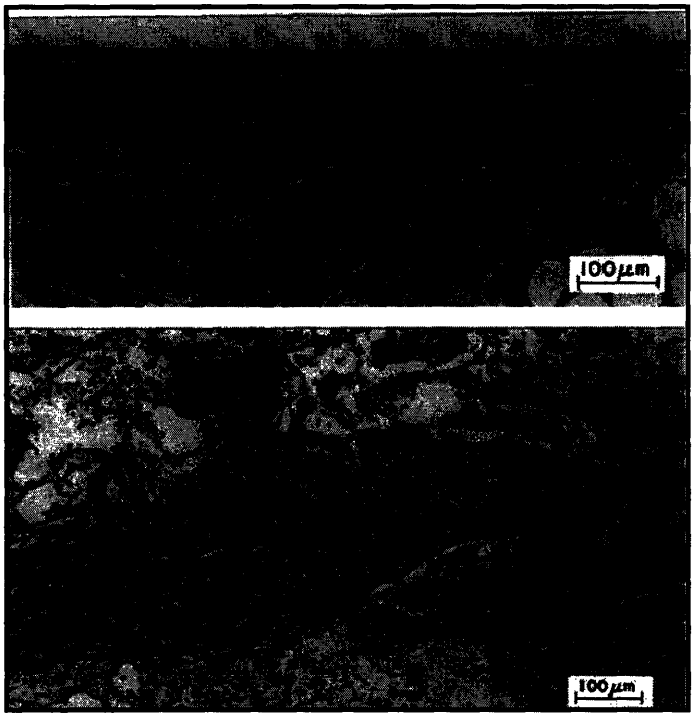

Figure 2.4: Fibroblast arrangement in wound site without (top) and with (bottom) scaffold (Troxel 1994)

In the top figure, the fibroblasts are very numerous and are contracting in a common plane. Conversely, in the bottom image, the myofibroblasts are much fewer, much more spread out, and have no distinguishable orientation.

2.3.3 Tissue Synthesis

Blocking contraction alone, however, is not sufficient to induce regeneration of tissue. In order to successfully cause regeneration, a scaffold must also allow for the synthesis of new stroma. There are many mechanical, biological, and chemical factors that affect the success of a scaffold. Figure 2.5 is a schematic of a typical collagen-GAG scaffold used for dermal regeneration.

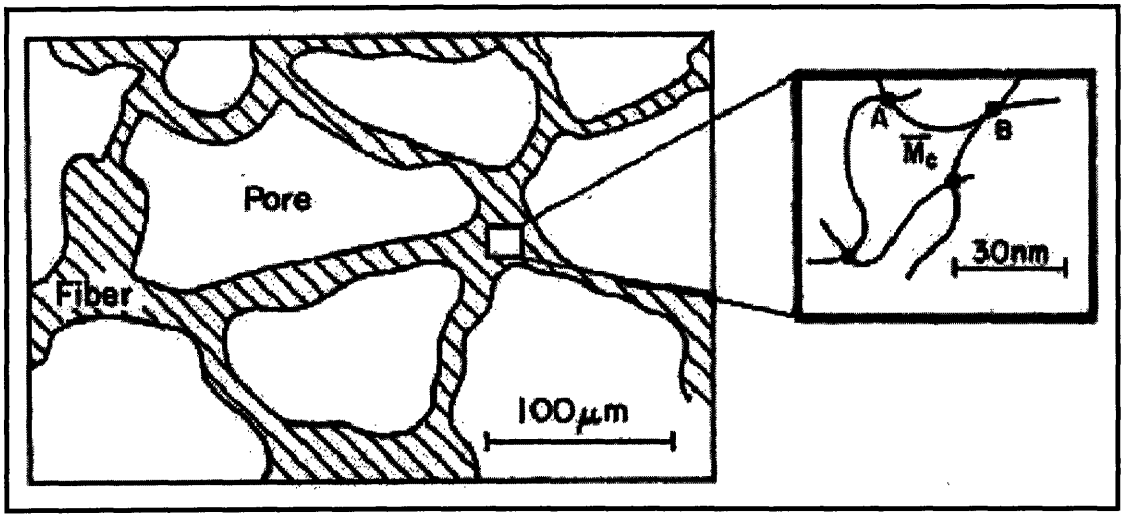

Figure 2.5: 2-D schematic of collagen-GAG matrix (Troxel 1994)

Some of the factors that affect the viability of a scaffold include pore size, pore volume fraction, rate of degradation, elastic modulus, and chemical composition. Pore size must fall within a certain range since pores that are too small will not allow cells to migrate into the scaffold. On the other hand, since cells communicate with each other through the release and diffusion of growth factors and other proteins, pore sizes that are too large inhibit the amount of intercellular contact that can exist. Similarly, if the pore volume fraction is too large, the amount of surface area on which cells can attach will be small compared to the amount of empty space. In this case, even if cells can migrate in through the large pores, the low surface area will make it difficult for them to find an available site to attach to. Conversely, if the pore volume fraction is too small, there will be too many struts in the matrix, which will prevent cells from migrating deep into the scaffold and only the edges of the scaffold will be populated. The degradation rate of the scaffold also plays a role since if the matrix degrades too fast, it will not block contraction long enough for new tissue to be synthesized and scar tissue will form instead. Also, if the degradation rate is too slow, it will physically hinder the synthesis of new tissue. The rate of degradation is typically controlled by changing the amount of cross-linking between collagen fibers in the collagen-GAG matrix. The stronger and more cross-linking there is, the longer the half-life of the scaffold. The chemical composition of the scaffold is also important as the proper integrins and amount of glycosaminoglycans must be balanced in order for the scaffold to be viable. Finally, the elastic modulus must be

within a certain range since the cells can only provide a certain amount of force and will not attach properly to the matrix if they cannot contract (Yannas 1989).

2.3.4 Other Factors Involved in Regeneration

In addition to preventing scar tissue formation, collagen-GAG scaffolds also promote regeneration in many tissues in the body that simply do not heal when damaged. For example, while the meniscus and nerve axons do not spontaneously heal when damaged, it is possible to induce regeneration of these organs and tissues through the introduction of scaffolds. The implantation of a scaffold gives these tissues a framework on which cells can migrate into the wound site and begin to generate new tissue. As such, different scaffold geometries and compositions are used depending on the kind of tissue being regenerated. For example, a nerve scaffold would consist of a cylindrical tube shaped scaffold to be implanted between the severed ends of a damaged axon, and a partially crystallized scaffold would be used in an area where there is the need to regenerate bone and cartilage. Thus, collagen-GAG scaffolds have a variety of current medical applications and warrant a more in depth characterization for future use and development.

2.4 Effect of Mechanical Properties of Environment on Cells

Cells respond not only to the chemical and biological properties of their environment but also the mechanical properties of their surroundings. For example, cells prefer a stiff environment to a soft environment (Figure 2.6).

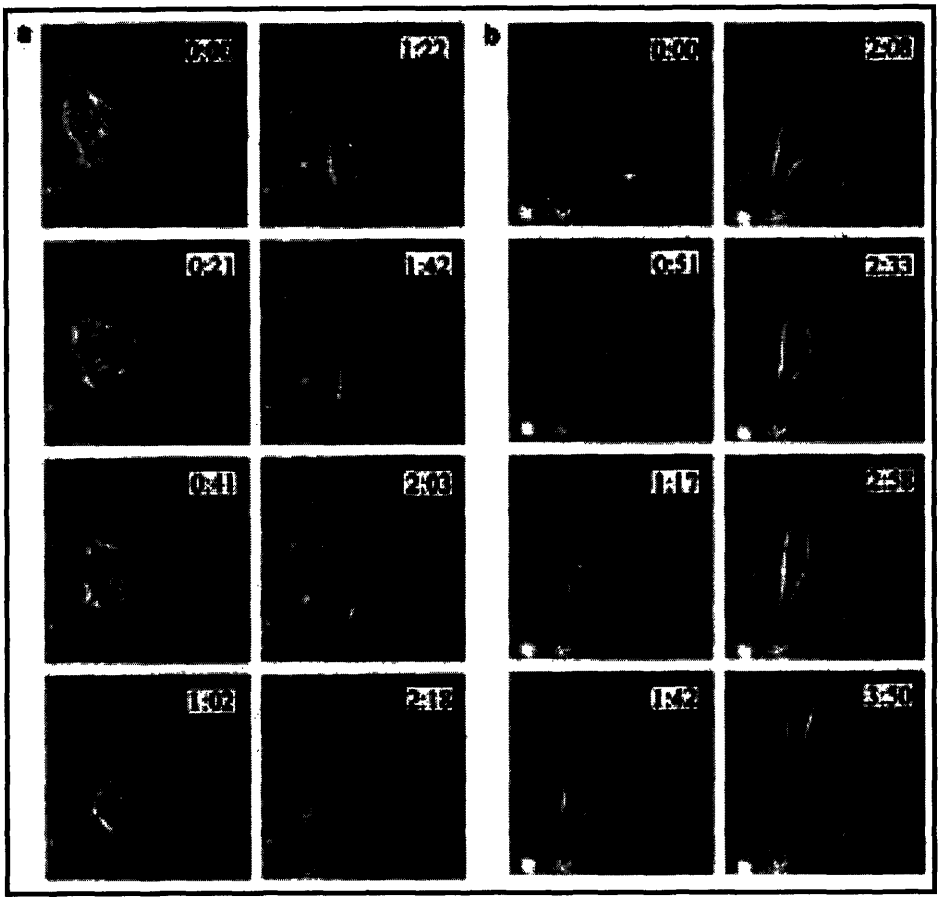

Figure 2.6: Image Sequence of cell on different stiffness substrates. Scale bar - 40μm. (Lo 2000)

The cell can determine the stiffness of the substrate and seeks out the stiffer substrate. When it is placed on the soft substrate, the cell migrates to the stiffer substrate and remains stationary. Interestingly, when the cell is placed on the stiffer substrate, it migrates toward the boundary of the soft substrate and remains on the stiff substrate but begins to migrate along the border of the two substrates.

As the scaffolds are designed to endure contraction by fibroblasts, it is important that the stiffness of the scaffolds be suitable for the attachment and activity of cells. For instance, in order for cells to properly attach and elongate on a matrix, the matrix must provide enough support for the cell (Figure 2.7). If the strut provides too much resistance, however, the cell will be forced to detach from the strut and will be unable to properly attach itself.

Figure 2.7: Cell (A) buckling struts of the matrix (B) while elongating. Scale-bar is 50μm. (Freyman 2001)

Thus, the stiffness of the collagen-GAG scaffold has an impact on the behavior of the cell and its response to its environment. Moreover, the mechanical properties of the matrix also affect the migration, attachment, and contraction of cells within the matrix (Harley 2006).

2.5 Mechanical & Geometric Model of Collagen-GAG Scaffolds

Collagen-GAG scaffolds are made primarily of collagen, and the current mechanical model for these scaffolds revolves around the hyperelastic model of networks of collagen fibers (Bischoff 1999). Interactions between cells and scaffolds, however, occur on the individual cell and individual strut level. Nevertheless, although we are primarily concerned with the mechanical properties of individual collagen fibers, because we cannot easily isolate individual collagen strands for mechanical testing, it is necessary to first develop an understanding of the macroscopic properties of the matrix as a whole.

2.5.1 Strain & Stress

Engineering strain is defined as the change in length of a specimen divided by the initial length of the material. If l is the current length of the specimen and l_0 is the initial length of the specimen, then the engineering strain, ε, is:

$$\varepsilon = \frac{l - l_0}{l_0} \tag{2.1}$$

Engineering stress is defined as the applied load divided by the initial cross-sectional area of the specimen. If P is the load being applied to the specimen and A_0 is the initial cross-sectional area of the specimen, then the stress, σ, is:

$$\sigma = \frac{P}{A_0} \tag{2.2}$$

In linear elastic materials, the relationship between stress and strain is:

$$\sigma = E\varepsilon \tag{2.3}$$

where E is a constant called the Young's Modulus or the Modulus of Elasticity. However, many networks of structural proteins or fibers in the body such as the extracellular matrix cannot be modeled as linear elastic materials and thus, require a more complex mechanical model.

2.5.2 Geometric Model

In order to develop a more complex mechanical model for the collagen-GAG matrix, an understanding of the geometric arrangement of collagen fibers within the scaffold is needed. Collagen-GAG scaffolds are a porous matrix of collagen fibers with glycosaminoglycans bonded to the collagen fibers. Generally, there is a pore volume fraction of at least 99% with a pore diameter ranging from 20 to 120 micrometers. In the scaffolds used to regenerate skin, the pores are oriented in a random manner in order to disorient the myofibroblasts when they contract and decrease the macroscopic contractile force. In scaffolds used for other purposes, such as nerve regeneration, directional pores may, however, be desirable. Figures 2.8 is a 3-D image of a collagen-GAG scaffold and figure 2.9 is an image of a cross sectional slice of a scaffold.

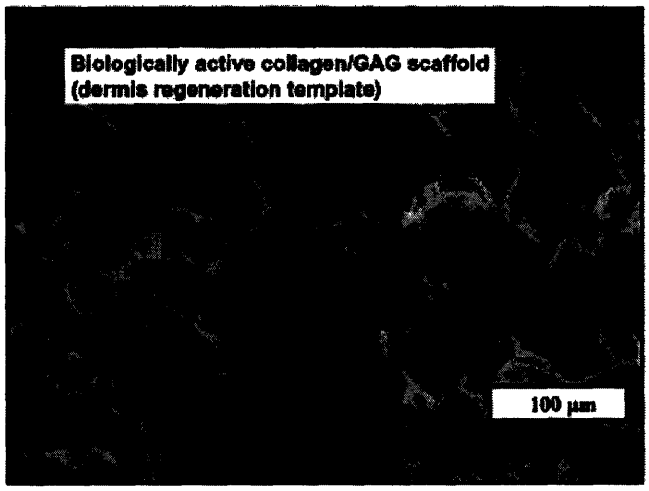

Figure 2.8: Scanning electron microscope image of a collagen-GAG scaffold (Yannas 2001)

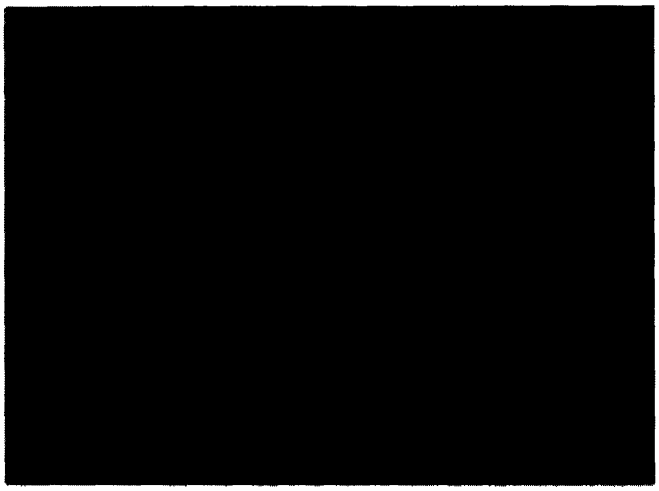

Figure 2.9: Cross sectional image of collagen-GAG scaffold (scale bar = 100µm) (Freyman 2001)

2.5.3 Hyperelastic Model of Collagen Matrix

The prevailing mechanical model for a collagen matrix under uniaxial tensile loading is the hyperelastic model, which consists of a primary non-linear stress-strain profile as well as a secondary linear stress-strain profile (Bischoff et al. 1999). The first part of the stress-strain curve is attributed to the geometric shifting of collagen fibers as they align themselves parallel to each other in the direction of loading. Although some fibers will be stretching, others are simply bending or becoming aligned with the direction of the applied load. Thus, initially, it takes very little force to cause an incremental change in length of the specimen, but as more and more fibers align, it takes more and more force to incrementally change the length of the matrix, which results in a non-linear curve. After all of the fibers have aligned, the stress-strain profile becomes dominated by the stretching of collagen fibers, which follows a traditional linear elastic stress-strain profile.

The collagen-GAG scaffolds will have to be tested in bulk since it is not feasible to test individual collagen fibers. Hence, it will be necessary to keep in mind the hyperelastic character of a matrix of collagen fibers. In order to test the mechanical response of individual fibers, testing must be done in a way that the specimen will reach the linear elastic region of the stress-strain curve where the fibers themselves are stretching rather than the simple geometric rearrangement of fibers in the network that occurs in the non-linear regime.

2.6 Viscoelastic Models & Determination of Linear Viscoelasticity

The primary concern of this thesis is to begin development of a viscoelastic model for collagen-GAG matrices and more specifically the collagen fibers themselves. Viscoelastic behavior refers to the response of a material to loading over time. Creep is the phenomenon by which materials when held at a constant stress achieve an initial strain and then over time continue to deform even more. In the case of a polymer, creep is caused by the slipping of molecules over time as a result of a constant applied load (Ashby & Jones 1996). Similarly, when a viscoelastic specimen is stretched to a particular strain level and held over a period of time, the stress required to hold the specimen at that strain begins to lessen. This is called stress relaxation.

The viscoelastic properties of a material depend on a variety of factors including crystallinity, the melting temperature of the material and the temperature of the environment. In the context of such complexity, one simple classification of viscoelastic materials is the delineation between linear viscoleastic materials and non-linear viscoelastic materials. Linear viscoelasticity refers to the property that the strain response of a material over time is proportional to the applied stress at every time point and vice versa (Yannas 1974). Thus, in order to determine whether a material exhibits linear viscoelastic properties, either the creep response must be observed at several different stress levels in order to determine whether the strain response over time is proportional to the applied stress or the stress relaxation curve must be examined at several different strain levels to see if the stress response over time is proportional to the strain level.

2.7 Temperature Dependence of Material Properties & Design of Water Bath

The collagen-GAG scaffolds being investigated are designed for use in a hydrated environment in the body, which is at a temperature of approximately 37°C. Consequently, it is most important to determine the material properties of the scaffolds at this temperature. To this end, a water bath must be designed to regulate the temperature of the environment in which the specimen will be tested.

2.7.1 Temperature Dependence of Viscoelastic Properties

The properties of materials such as the Young's modulus, yield strength, and viscoelastic properties all change with temperature. Materials exhibit the greatest viscoelastic response in temperatures close to the glass transition temperature of the material when the material enters a leathery stage. Because of the low crystallinity of polymers and their low melting point, polymeric materials tend to exhibit creep properties even at low temperatures. As the temperature increases, bonds between molecules are less stable and it becomes easier for molecules to slip past each other, which contributes to a material's creep response. Figure 2.10 shows the creep response of a material at different temperatures. Increasing the temperature produces a similar effect as increasing the amount of stress; in both cases, the rate of creep increases.

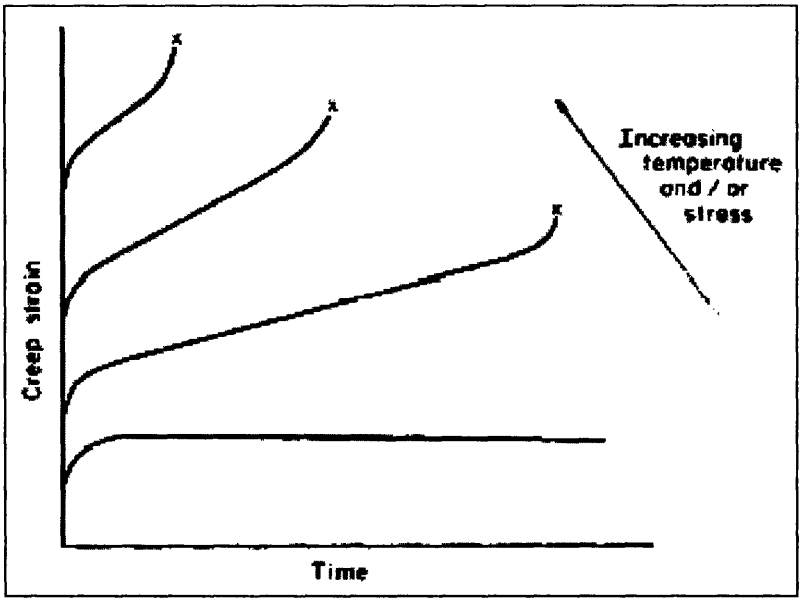

Figure 2.10: Creep vs. time curves at different temperatures (Ashby & Jones 1996)

2.7.2 Water Bath Design

The mechanical testing apparatus has already been fitted with a hydration chamber to allow testing of specimens in a hydrated environment. The purpose of the water bath is to maintain the liquid in this chamber at a constant temperature of 37°C for the duration of the tests. The basic components necessary for such a water bath include a thermocouple, a temperature controller, a solid-state relay, a heater, and something to ensure that there isn't a temperature gradient throughout the liquid (Omega®).

Additionally, water baths have been used in similar applications in previous research and can provide insight into designing a successful system.

One particular setup used a temperature regulator/mixer from Brinkman Instruments to test the creep properties of bone samples at six different temperatures and check for temperature dependency of the creep mechanism (Bowman 1997). The temperature regulator maintained the temperature within .1°C of the specified temperature and a mixer ensured an even temperature distribution throughout the apparatus. Such a setup is ideal for testing samples since it is a removable apparatus that can be installed in a pre-existing machine and doesn't require integrated design into the testing apparatus itself.

Controlling the temperature of small volumes can also be very difficult. Thus, another design aspect employed by Bowman (1997) was to maintain a reservoir of liquid at constant temperature and continuously circulate water between the reservoir and the chamber containing the sample being tested. This design provides a more accurate means of maintaining the temperature of the small volume of liquid in the test chamber through the use of a large volume reservoir that has a stable temperature.

3. Methodology & Materials

The steps involved in this thesis included the fabrication of collagen-GAG scaffolds, the preparation and mechanical testing of scaffold samples, and the design and implementation of the water bath. In order to manufacture collagen-GAG scaffolds, a slurry of chemical components was mixed, degassed, frozen, and the liquid sublimated to form a dry collagen-GAG scaffold. Specimens then needed to be cut, and for hydrated tests, they need to be placed in 1x phosphate buffer solution (PBS) for at least 12 hours prior to testing. 1x refers to the standard dilution of PBS that you're supposed to use, which is often prepared from a 10x solution of PBS that is readily available for purchase. Stress relaxation tests were performed using a Zwick mechanical testing machine on these specimens at room temperature. The design of the water bath occurred independently in order to be implemented to allow for testing at 37°C.

3.1 Fabrication of Scaffolds

The first stage of the project was to fabricate scaffolds to be used in the mechanical tests. Fabrication of these scaffolds began with making a slurry of collagen and glycosaminoglycans dissolved in acetic acid, which was then degassed and frozen. The frozen slurry was then placed in a vacuum to allow sublimation of the ice crystals which leave behind pores within the collagen-GAG network, creating the scaffold.

3.1.1 Making Slurry

Slurry was prepared from type I microfibrillar bovine tendon collagen (Integra LifeSciences, Inc., Plainsboro, NJ) and chondroitin 6-sulfate (Sigma-Aldrich Chemical Co., St. Louis, MO), which was the glycosaminoglycan used in these scaffolds, which is dissolved in .05M acetic acid. The standard protocol used is described in O'Brien et al. 2003.

The process began with dissolving the collagen in .05M acetic acid in a chamber cooled to 4°C with a Brinkman model RC-2T cooling system (Brinkman Co., Westbury, NY) using a blender (Ultra Turrax T18 Overhead blender, IKA Works, Inc., Wilmington, NC) at 15,000 rpm for 90 minutes (Figure 3.1). The chondroitin 6-sulfate was simultaneously dissolved in a beaker of acetic acid using a stir bar. The dissolved chondroitin 6-sulfate was then added to the collagen mixture using a peristaltic pump to regulate the flow to 120mL of liquid per 15 minutes while moving the blender around in the slurry to ensure even distribution of the chondroitin 6-sulfate. The slurry was then blended for an additional 90 minutes at 15,000 rpm. Throughout this entire process, the chamber was maintained at a temperature of 4°C.

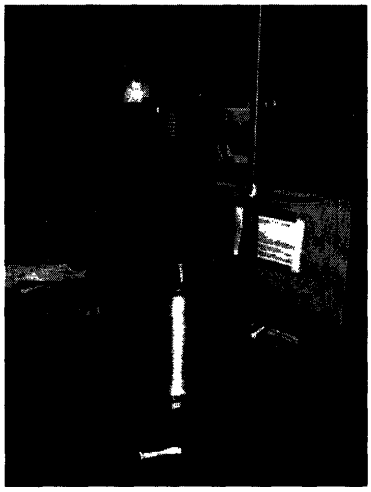

Figure 3.1: Mixing chamber with attached cooling system and blender

Once the slurry had finished mixing, it was completely transferred into a vacuum flask where it was degassed using a vacuum pump for at least 60 minutes or until bubbles were no longer present in the solution. The slurry was stored in a capped bottle (Figure 3.2) at 4°C until it was ready to use.

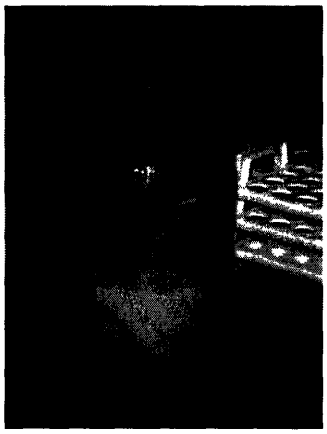

Figure 3.2: Capped bottle containing type I collagen-GAG slurry

3.1.2 Freeze-Drying

Once the slurry was made, scaffolds were prepared at most 3 at a time in 5 in. x 5 in. stainless steel pans (Figure 3.3). These pans contained the slurry that were placed in the freeze dryer (Genesis, VirTis, Gardiner, NY) (Figure 3.3), which would freeze the scaffolds and then create a vacuum to sublimate out the frozen ice crystals.

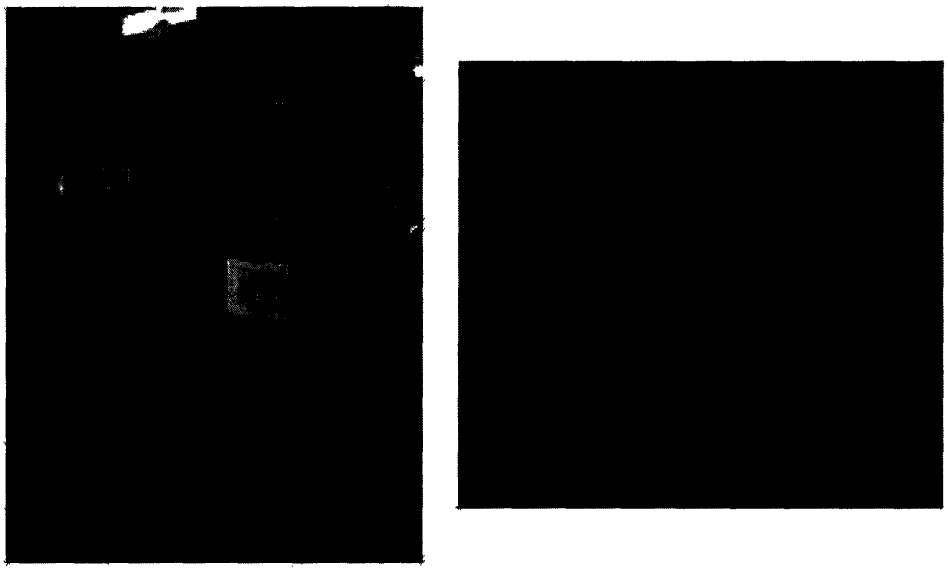

Figure 3.3: Freeze dryer and stainless steel pan used to fabricate scaffolds. Scale bar = 1.25"

Before making a batch of scaffold, the slurry had to be degassed again for between 30 to 90 minutes using a vacuum pump to remove excess air bubbles. The stainless steel pans were then wiped clean with acetic acid and slurry was pipetted into each pan. Air bubbles created during pipetting were dragged to the sides of the pan since the edges of each scaffold would be cut off.

The pans were placed in the freeze dryer and the freeze drying program was initiated. The process consisted of an initial freezing process in which the temperature of the chamber was steadily ramped from 20°C to -40°C over a period of 65 minutes. This protocol has been shown to produce average pore sizes of approximately 96 μm with a porosity of 99.5% (O'Brien 2003). The entire chamber was then held at -40°C for at least another 60 minutes before the vacuum was turned on.

Once the freezing program had finished running, the vacuum on the freeze-dryer was manually turned on. The strength of the vacuum in the chamber fluctuated between 400 to 700 mTorr. Once the vacuum strength reached a plateau, which was usually at around 400 mTorr, the temperature of the chamber was raised to 0°C and the freeze-dryer was allowed to run for at least 17 hours. Figure 3.4 is a phase diagram of water, which also illustrates the pathway that the water takes as it freezes and then is sublimated at low pressure.

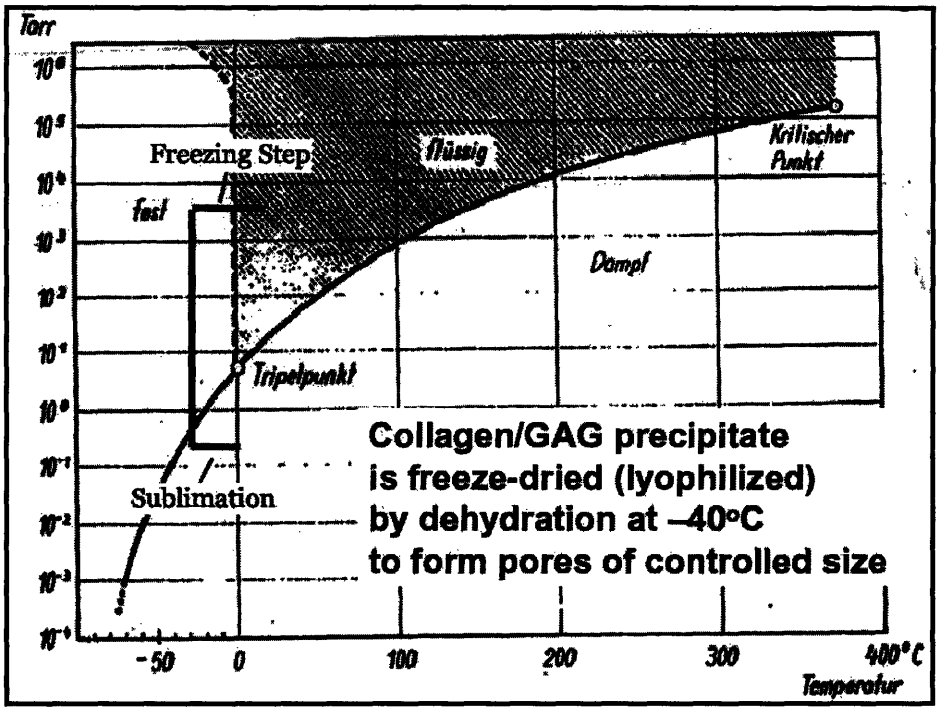

Figure 3.4: Phase diagram of water used to monitor freeze-drying with pathway of acetic acid during collagen-GAG scaffold fabrication (Yannas 2001)

This process produced sheets of collagen-GAG scaffold, which were 5" x 5" in area and were ~3.5 mm thick. The scaffolds were removed from the pan using stainless steel forceps and stored in envelopes made of heavy duty aluminum foil that were placed in a desiccator at room temperature.

3.2 Preparation of Specimens for Mechanical Testing

In preparation for mechanical testing, strips of scaffold needed to be cut from the sheets of collagen-GAG scaffold. The cut specimens were 25 mm long and 20 mm wide, and were cut from the scaffold sheets using a razor blade. Because of the tendency of the scaffold to tear when the blade was dull, a new razor blade had to be used after every 4 to 5 cuts. To ensure that cuts were made straight, the strips were measured off at either end, and then a ruler was laid across the scaffold to act as a cutting guide for the razor blade. This required slight pressure on the ruler without applying too much force so as to crush the scaffold.

Additionally, some of the tests were performed using hydrated specimens. Samples used in hydrated tests had to be soaked in 1x PBS for at least 12 hours before testing. This was to ensure that the scaffolds had soaked up as much liquid as possible before they were used in the tests. Hydrating the scaffolds was done in 6 well plates (Figure 3.5).

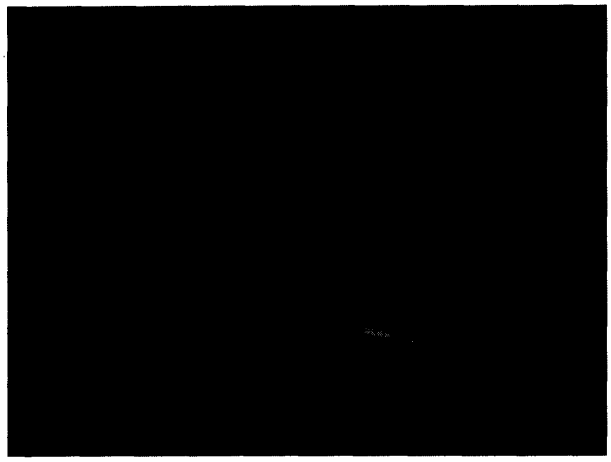

Figure 3.5: 6-well plate used to hydrate collagen-GAG specimens

The samples were placed in the wells, and 1x PBS was added around the edges of the scaffold to allow the matrix to slowly soak up the liquid. Adding the liquid directly on top of the scaffold would cause local deformations to the scaffold that could cause it to warp and lose its porous structure. Once the PBS had begun to soak into the specimens, the wells were filled to at least 3 times the thickness of the scaffolds with PBS without ever adding PBS directly on top of the scaffold so as to avoid crushing it. They were then allowed to sit undisturbed for at least 12 hours. It was found, however, that although the scaffolds could be allowed to sit in PBS for several days before testing, they began to breakdown over time, and by the 7^{th} day after hydrating, they were too soft to handle with a spatula.

3.3 Mechanical Testing

The next stage in this project was to perform the mechanical tests on both dry and hydrated samples using a Zwick machine (Zwick Z2.5/TSIS). Simple tension tests of dry and hydrated specimens as well as stress relaxation tests at different strain levels for both dry and hydrated samples all had to be performed in order to determine whether collagen-GAG scaffolds exhibit a linear viscoelastic behavior.

3.3.1 Testing Apparatus, Setup, and Software

The Zwick machine was equipped with a 20 N load cell, which had a resolution of .2 mN. It was also outfitted with stainless steel grips used for tensile loading, a clear acrylic hydration chamber, and other attachments and pins for assembling all of the parts. Figure 3.6 shows the setup of the machine that was used for both dry (left) and hydrated (right) tension and stress relaxation tests.

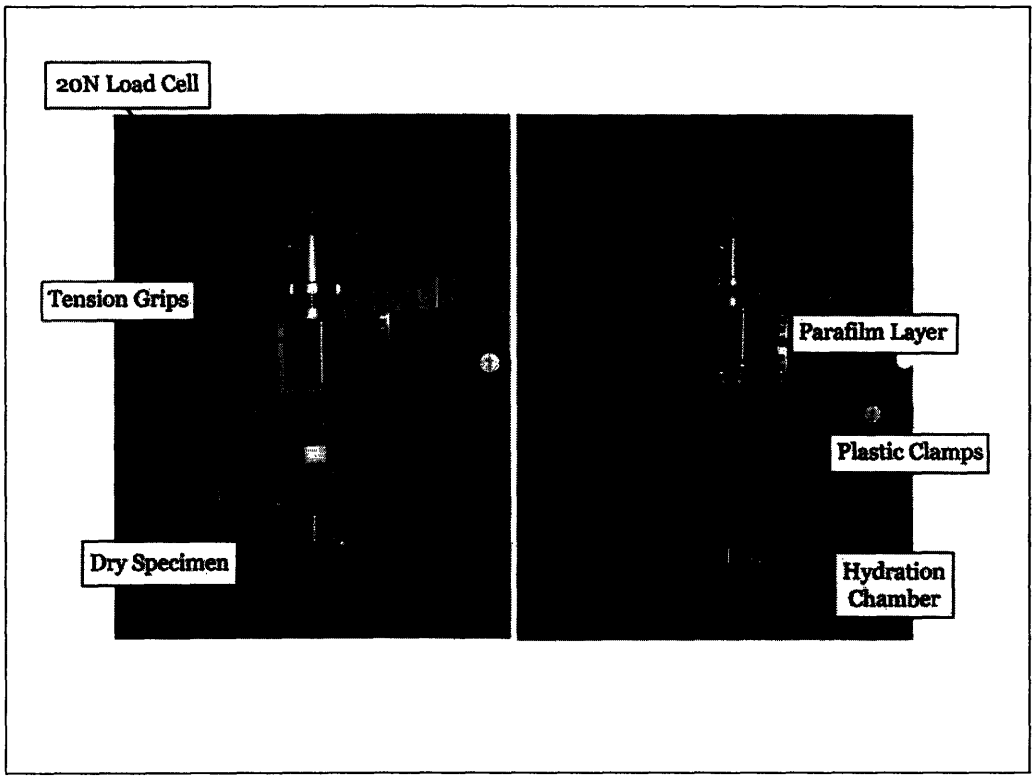

Figure 3.6: The setup for dry (left) and hydrated (right) tension and stress relaxation tests

One complication that arose in the use of the hydration chamber is that the chamber leaked slowly. For the hydrated stress relaxation tests that were being performed, this presented an issue because of the change in buoyant force that resulted from the leaking chamber. Forces attained in the stress relaxation tests were on the order of 2 to 10 mN. By using Archimedes' principle, which states that the buoyant force is equal to the weight of the volume of the water displaced by a submerged object, it was calculated that a decrease in water level of 1mm would cause an extra 1mm of the testing apparatus to come out of the water and decrease the buoyant force by about 1.37 mN. Consequently, any changes in water level would have significant results on the stress relaxation tests. In order to try to compensate for this problem, before every test, a sheet of parafilm was applied over the front of the hydration chamber to try to provide an extra seal before the front panel was clamped on. The success of this solution was limited but when performed properly could prevent the leaking.

Dry specimens were loaded into the tension grips as shown in Figure 3.7. The specimen was placed onto one side of the grips, and when it was positioned properly, the other half of the grips were attached on by screws and tightened using a hex wrench. Loading hydrated specimens proved to be a much larger challenge because once the hydrated specimens were taken out of water, they became extremely slippery, amorphous, and hard to work with. As a result, loading of hydrated samples into the tension grips was done in a tray filled with 1x PBS (Figure 3.7) and a spatula. The tray was filled with just enough liquid to cover the bottom half of the tension grips so that some of the specimen remained out of the water when loading. This prevented the specimen from moving around due to the water currents created by movement of the spatula or when trying to sandwich the specimen between the two halves of the tension grips.

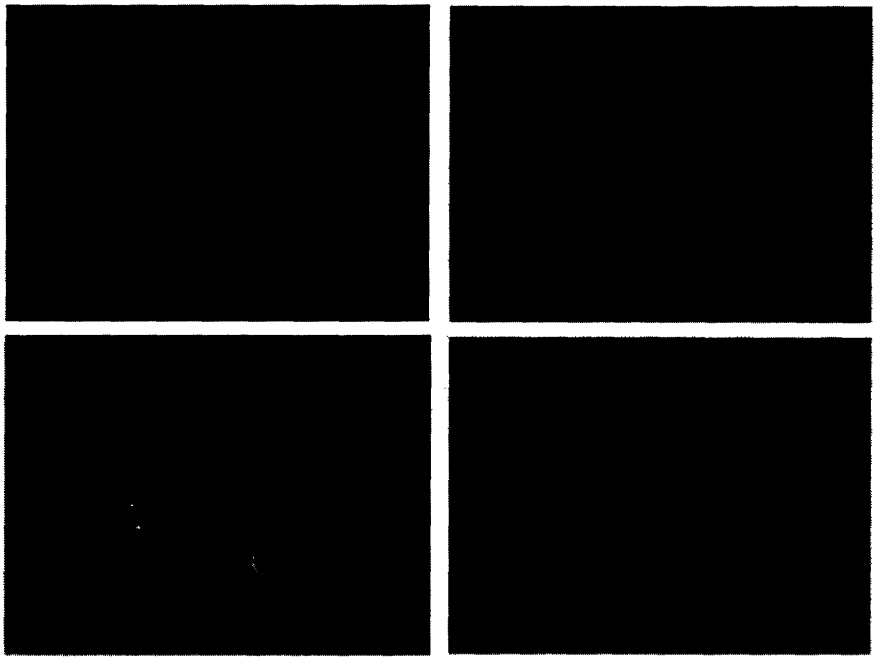

Figure 3.7: Loading of dry specimens into tension grips, (lower right) tray filled with 1x PBS used in loading hydrated samples into tension grips.

The width and thickness of the dry specimens were measured before loading them into the tension grips, but the initial gage length and all of the dimensions for the hydrated specimens were measured after being loaded into the grips.

The testing software that went along with the testing machine was called TestXpert. Using this program, test programs for simple uniaxial tension tests as well as stress relaxation tests were created. For the tension tests, the initial gage length and dimensions of the specimen would have to be entered into the program, but once this was completed, the software would calculate the strain and measure the associated stress on its own. Once the stress-strain curves for both hydrated and dry collagen-GAG scaffolds were obtained, the stresses which corresponded to the strain levels that the stress

relaxation tests were to be performed at were obtained. In the programs for the stress relaxation tests, the machine was told to go to the stress that corresponded to the desired strain level and to hold at that position for 5 hours while the stress was monitored. The reason for programming the tests this way was to make it easier to compare the stress relaxation test trials that were performed at the same strain level as well as to try to minimize variation in measuring the initial gage length when loading the specimen into the machine.

3.3.2 Tension Tests

Simple uniaxial tension tests were performed on both hydrated and dry specimens to obtain a stress vs. strain curve for these scaffolds. Ultimately, the goal was to run stress relaxation tests on specimens in order to determine whether or not the material exhibits linear viscoelastic behavior. In order to standardize the initial stress of the stress relaxation curves, it was decided that tension tests should be run in order to determine the stresses that corresponded to the strain levels at which the stress relaxation tests would be performed. This would also help to mitigate the effects of measurement error when measuring the initial gage length of the specimens, which proved to be difficult because of the low stiffness of the hydrated scaffolds.

The stress-strain data from three dry specimens and four hydrated specimens were averaged to develop a stress-strain curve for both dry and hydrated collagen-GAG scaffolds. Based on these curves it was decided to perform the stress relaxation tests at 6%, 9%, and 12% strains in the hydrated specimens and to perform stress relaxation tests at 9%, 12%, and 15% strains in the dry specimens. The goal was to choose strains that lay in a linear portion of the stress-strain curve to ensure that the stress relaxation was due to the relaxation of collagen fibers that had been stretched as opposed to fibers that had simply been bent or whose geometric positioning had been changed (see section 2.5.3).

This method for standardizing the stress relaxation tests, however, was not developed until virtually all the hydrated samples were used up, so most of the hydrated stress relaxation tests were performed at a wide variety of initial stresses but approximately at the desired strains.

3.3.3 Stress Relaxation Tests

Three trials of stress relaxation tests were performed on dry specimens at each of the chosen strain levels (9%, 12%, and 15% strain). The specimens were loaded into the machine and the test program was allowed to run for 5 hours. Most of the stress relaxation tests of hydrated specimens were performed at a variety of different initial stress levels (see section 4.4). The hydrated tests presented challenges because of the leaking of the hydration chamber as well as the sensitivity of the tests. Because the observed stresses were on the order of milliNewtons, many irregularities in the stress relaxation curves arose, and it was often impossible to explain their cause. Any slight disturbance to the table that the testing apparatus was resting on, loud noises from other machines in the lab, or even the cleaning machines that the janitors used to clean the halls could have contributed to disturbances that disrupted the stress relaxation tests.

In order to account for some of these considerations, some tests were observed in order to try to explain any discrepancies in the graphs, but it was impossible to watch over every single test and inevitably many of the graphs have inexplicable variations. Moreover, the leaking of the chamber was closely monitored when possible, and tests in which leaking seemed to be a major factor had to be thrown out.

3.4 Water Bath Design

The last component of this thesis was the design and implementation of a water bath to control the temperature of the hydration chamber in which stress relaxation tests were being performed. The water bath needed to fulfill several functional requirements including maintaining the temperature of the hydration chamber, fitting within space in and around the testing apparatus, being compatible with the electrical capabilities of the room, and being built under a budget of $1,000. Based upon these considerations, two designs for a water bath were proposed for examination.

3.4.1 Functional Requirements

The water bath needed to be able to operate at temperatures within the range of 20°C to 50°C since 20°C is approximately the lower bound of room temperature while collagen begins to denature at about 50°C. Since the creep properties of collagen vary exponentially with temperature (Crandall & Dahl 1999), it was necessary to control the temperature within .5°C of the specified temperature. The hydration chamber had a volume of approximately 72.75 cubic centimeters, so the temperature control system had to be able to maintain the temperature of that volume of liquid at the desired temperature.

In addition to being able to adequately control the temperature, there were space restrictions on the system as well. The hydration chamber had very little room for parts inside it and there was limited amount of space around the Zwick machine to access the hydration chamber while it was loaded in the machine. The only sources of electrical power were 120V wall sockets, so the system also had to be compatible with that electrical input. Finally, the aim was to build a system that would cost less than $1,000 if possible.

Moreover, a quick call to Omega Engineering Inc. (Stamford, CT) revealed that a basic temperature control system such as this would need to at least consist of a thermocouple used to determine the temperature of the water, a temperature control unit, which is hooked up to a solid state relay and a heater, which would be used to heat the water. Other design considerations that were mentioned are also that the power of the heater must be chosen carefully so that significant temperature gradients do not form within the water bath itself.

3.4.2 Water Bath Design #1

In light of these functional requirements, one of the proposed designs would directly control the temperature of the hydration chamber by inserting the thermocouple and the heater directly into the hydration chamber itself and connecting them to the temperature control unit in a simple feedback loop. Figure 3.8 shows a flowchart of the system.

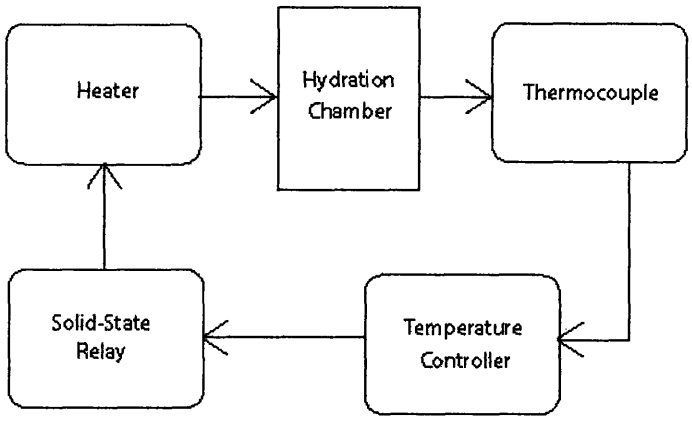

Figure 3.8: Flowchart of water bath design #1

The main advantage of this design was its simplicity. Additionally, because the thermocouple and the heater would interact directly with the hydration chamber, the system would respond much quicker to changes in temperature in the hydration chamber. There were some drawbacks, however, which included the fact that the chamber might be too small to adequately accommodate the thermocouple and heater. Moreover, it might be difficult to maintain such a small volume of liquid since turning the heater on for even a short while might cause a rapid increase in water temperature.

3.4.3 Water Bath Design #2

Another water bath design that provided an alternative to eliminate some of the deficiencies of water bath design #1 made use of a temperature controlled reservoir that would feed into the hydration chamber as was used by Bowman (1997). The schematic for such a design is shown in figure 3.9.

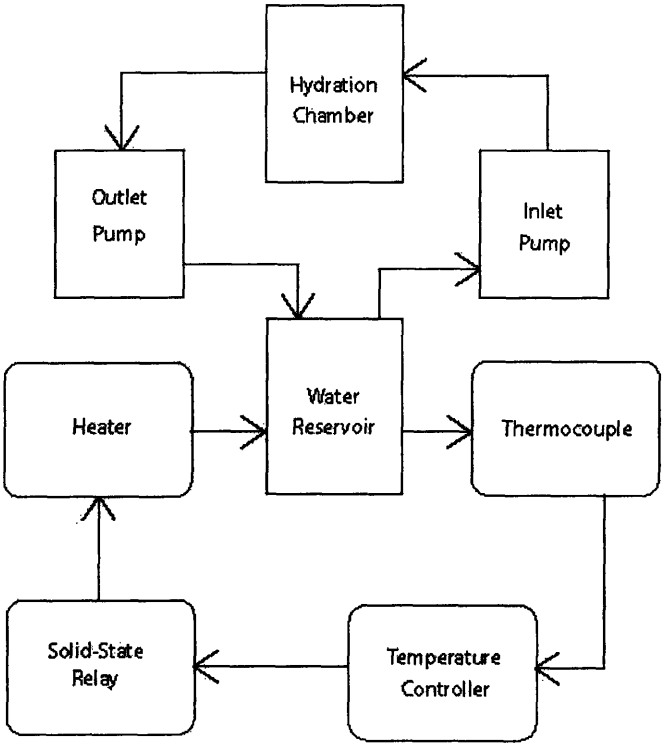

Figure 3.9: Flowchart of water bath design #2

The advantages of this design are that it is much easier to maintain a larger volume of liquid at a constant temperature. Also, because water from the reservoir is being pumped into the hydration chamber, there are much fewer parts that need to be able to fit around and inside the hydration chamber itself. This design is, however, significantly more complicated than design #1. Furthermore, there is less control over the temperature in the hydration chamber itself since the temperature controller is hooked up to the reservoir as opposed to the hydration chamber directly.

4. Data Analysis & Results

The data of interest collected in the tension and stress relaxation tests include the stress, strain, and test time. The Zwick mechanical tester can automatically collect and calculate the stress and strain from the dimensions of the specimens given, however, because of the external factors that influence the test results, especially in the hydrated tests, raw displacement and force data were exported from the test trials for analysis. Also, after careful evaluation of the two proposed water bath designs and research into

the system components, it was decided that water bath design #2 should be used to regulate the temperature of the hydration chamber.

4.1 Tension Tests of Dry Collagen-GAG Scaffolds

The purpose of tension tests on dry specimens was to establish a stress-strain curve for dry collagen-GAG scaffolds in order to determine the stresses which corresponded to the strains at which the stress relaxation tests would be performed. Data from the tension tests was normalized by arbitrarily calling the point at which the stress achieves .01N the zero point. The stress-strain curves that resulted from the 3 trials are graphed in figure 4.1.

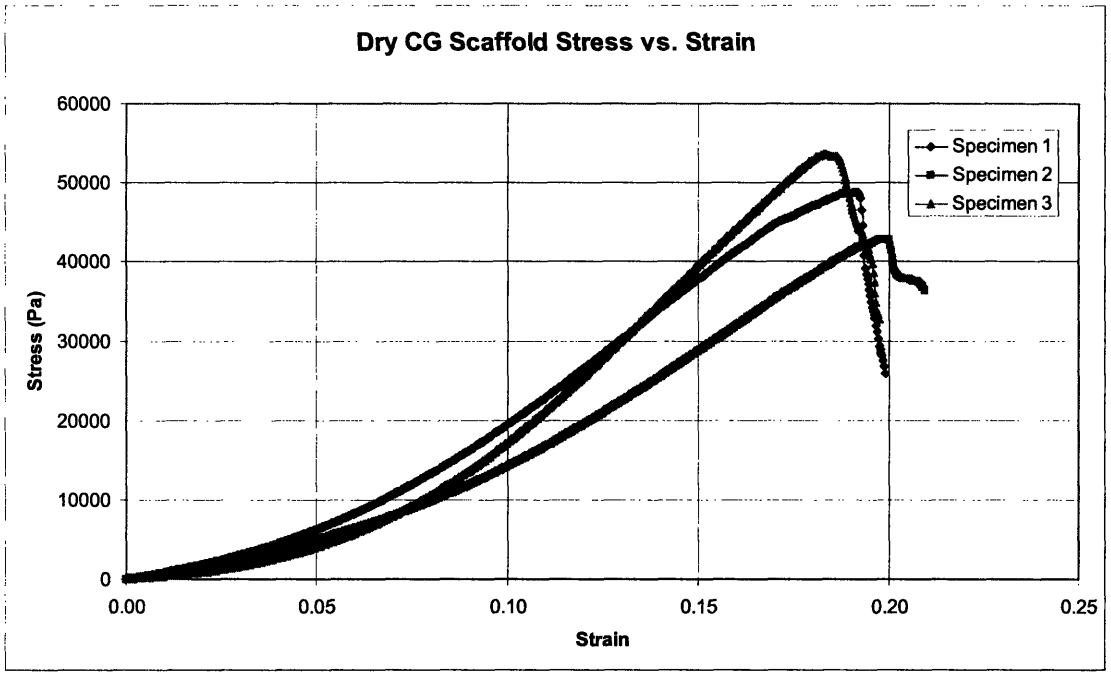

Figure 4.1: Stress vs. strain curves of dry collagen-GAG scaffold specimens

The dry collagen-GAG scaffolds exhibited hyperelastic behavior that is typical of collagen networks (see section 2.5.3). The scaffolds all tended to fail prior to reaching 20% strain. The average stress vs. strain along with error bars of 1 standard deviation above and below the average value are plotted in figure 4.2

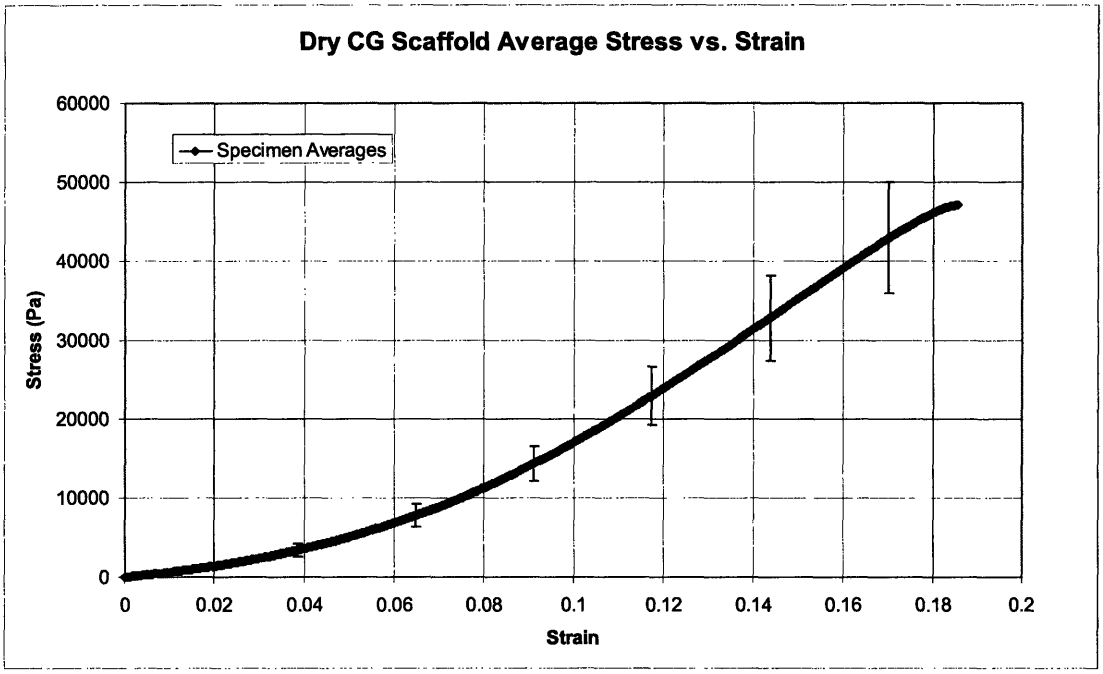

Figure 4.2: Average stress vs. strain curve of the three dry collagen-GAG specimens

The average stress vs. strain graph is clearly comprised of an initial nonlinear region and a subsequent linear region characteristic of hyperelastic materials. Based on the hyperelastic model, the secondary linear region is the region in which the struts of the matrix have aligned and are all beginning to elongate. Thus, the strain levels used in the stress relaxation tests should be chosen from this regime, which spans from approximately 9% strain to 16% strain. The values of stress that correspond to 9%, 12%, and 15% strain are 13950 ± 2210 Pa, 23825 ± 3810 Pa, and 35275 ± 5870 Pa respectively.

4.2 Stress Relaxation Tests of Dry Collagen-GAG Scaffolds

Stress relaxation tests were performed on dry collagen-GAG scaffolds at the 3 aforementioned strain levels. For each strain level, 3 specimens were tested for 5 hours in order to obtain a stress relaxation profile. The force and time data from the Zwick machine were gathered and the point at which the force reached a maximum was defined as the zero time point. Based on the dimensions of the different specimens, the stress for each specimen was calculated and the average stress relaxation profile at each strain level was graphed (Figure 4.3). The error bars indicate one standard deviation above and below the averaged curve.

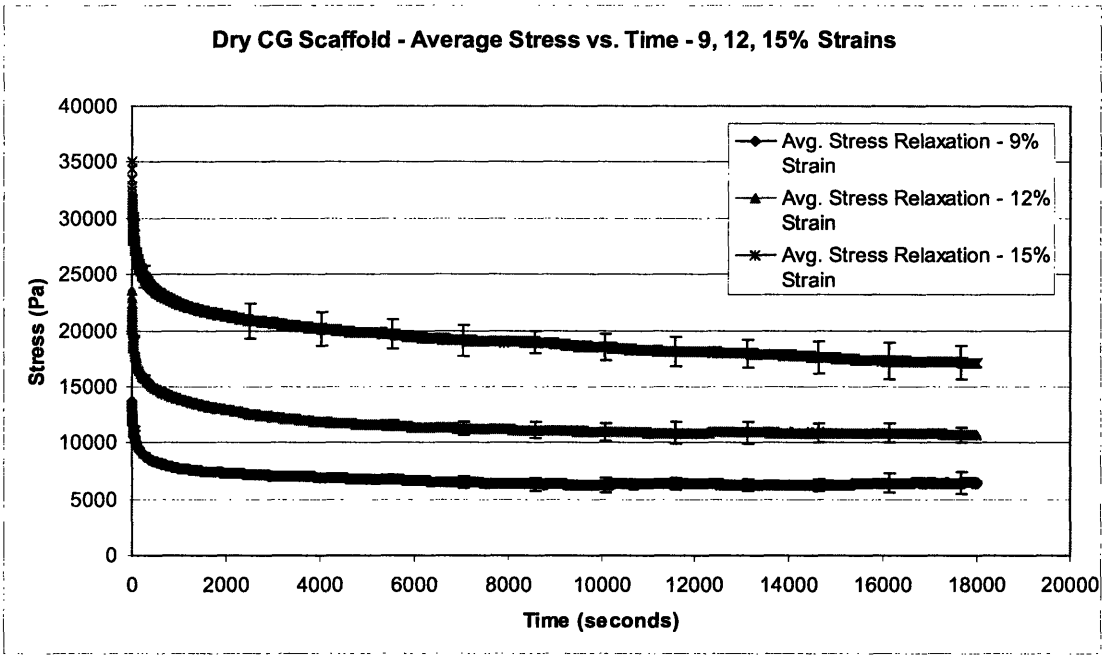

Figure 4.3: Average stress relaxation curves at 9, 12, and 15% strains

In order to determine whether the material exhibits linear viscoelastic properties, it is necessary to assess whether the stress relaxation response is proportional to the strain level. In the case of linear viscoelasticity, the viscoelastic modulus should be equal to the stress relaxation response divided by the strain (equation 4.1). If the material is not linear viscoelastic, the viscoelastic modulus would have some other form, perhaps exponential.

$$E(t) = \frac{\sigma(t)}{\varepsilon} \tag{4.1}$$

In order to test for linear viscoelasticity, each of the averaged stress relaxation curves was divided by the strain. If it was the case that the material was linear viscoelastic, the resulting curves should all lie on top of each other. The average relaxation modulus is plotted against time for each of the different strain levels in figure 4.4.

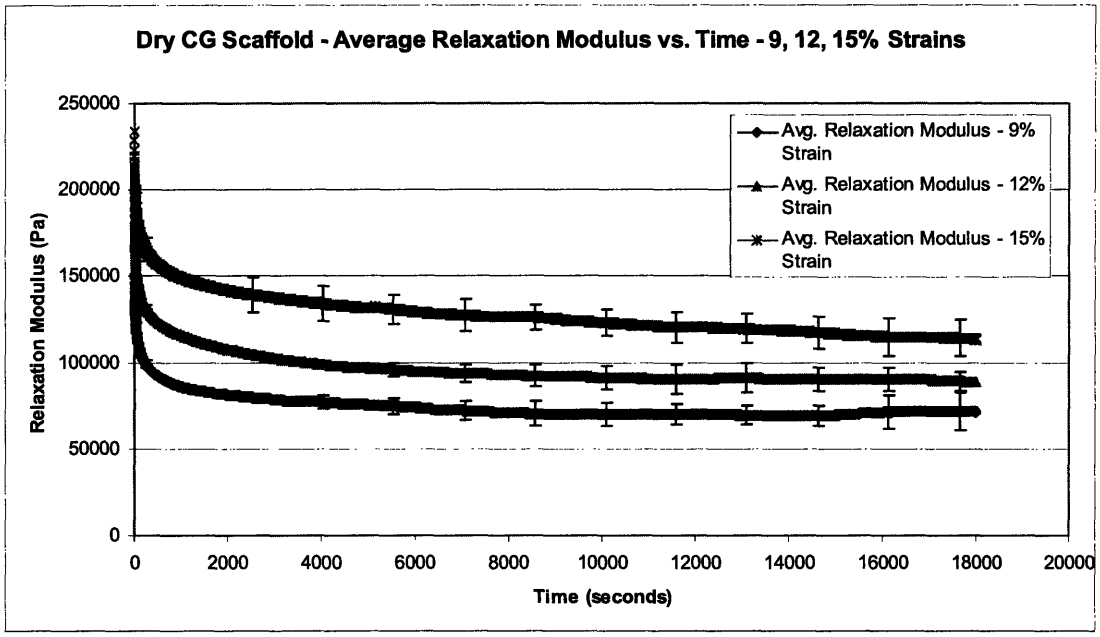

Figure 4.4: Average relaxation modulus at 9, 12, and 15% strains

From this graph, it is clear that the viscoelastic modulus do not lie on each other, and from the error bars, it is with at least 95% confidence that it can be concluded that the dry collagen-GAG scaffolds do not exhibit linear viscoelastic behavior. Thus, a more complex mathematical model needs to be developed in order to explain the viscoelastic behavior of these collagen-GAG scaffolds.

4.3 Tension Tests of Hydrated Collagen-GAG Scaffolds

The hydrated tests were performed much in the same way as the dry tests, however, the sensitivity of the hydration tests posed several problems. Since the hydration chamber was fixed to the bottom of the Zwick testing machine, as the tests were run, the grips and fixtures to which the specimens were attached would slowly begin to rise out of the water. This change in submerged volume of the fixtures contributed to a change in the buoyant force, which had to be accounted for in the data. Consequently, the first step in collecting data for tension tests was to create a baseline graph of the force vs. displacement of the machine with the hydration chamber set up but without any specimen. Any detected load would be attributed to the change in buoyant force. Figure 4.5 shows the results of this calibration.

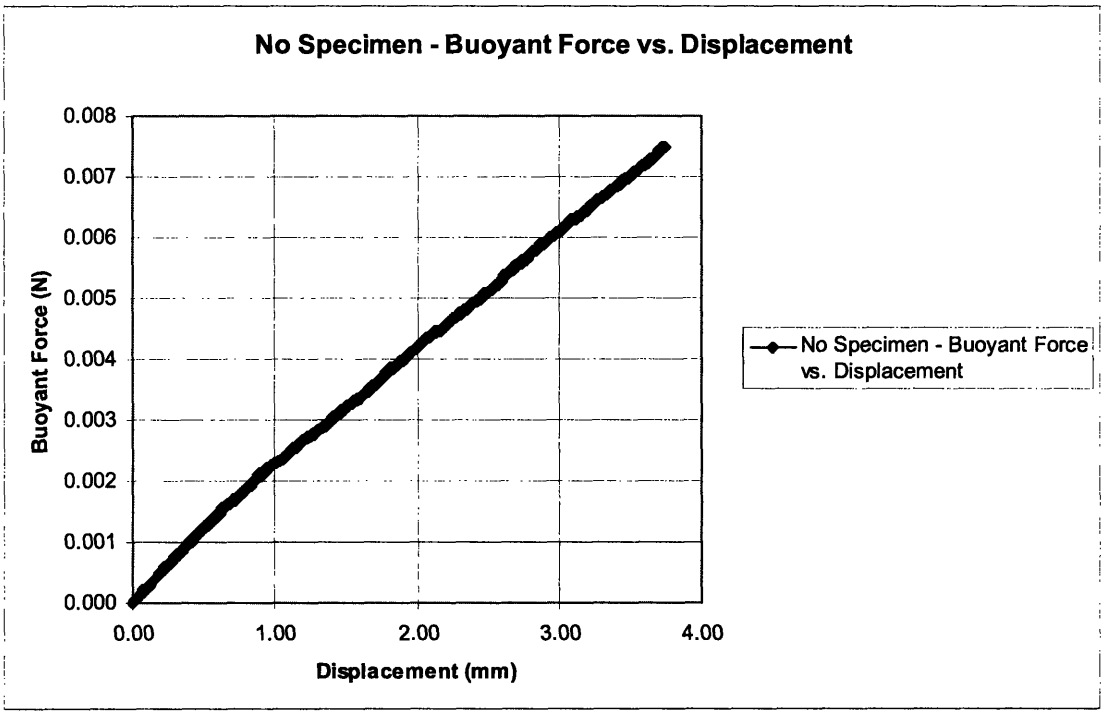

Figure 4.5: Buoyant force vs. displacement curve of machine without specimen

The graph is expected to have this linear shape because the part of the fixture that moves in and out of the water is a cylinder of constant diameter, which means that the rate of change of volume of submerged fixture is generally constant over the distance which the tension and stress relaxation tests would take place.

Because of the low forces required to stretch the hydrated samples as well as the fact that displacement of the fixtures would register a change in force, it was difficult to determine at the beginning of the stress-strain curves when the recorded force started being due to the resistance of the specimen to strain as opposed to just the change in buoyant force due to movement of the fixtures. Thus, in order to find the zero point of the data, the control curve was subtracted from each of the tension curves. The point at

which the resultant curve began to increase was taken to be the point at which the specimen started to stretch.

Similar to the dry tension tests, based on the dimensions of the specimens, the stress and strain were calculated and graphed (Figure 4.6).

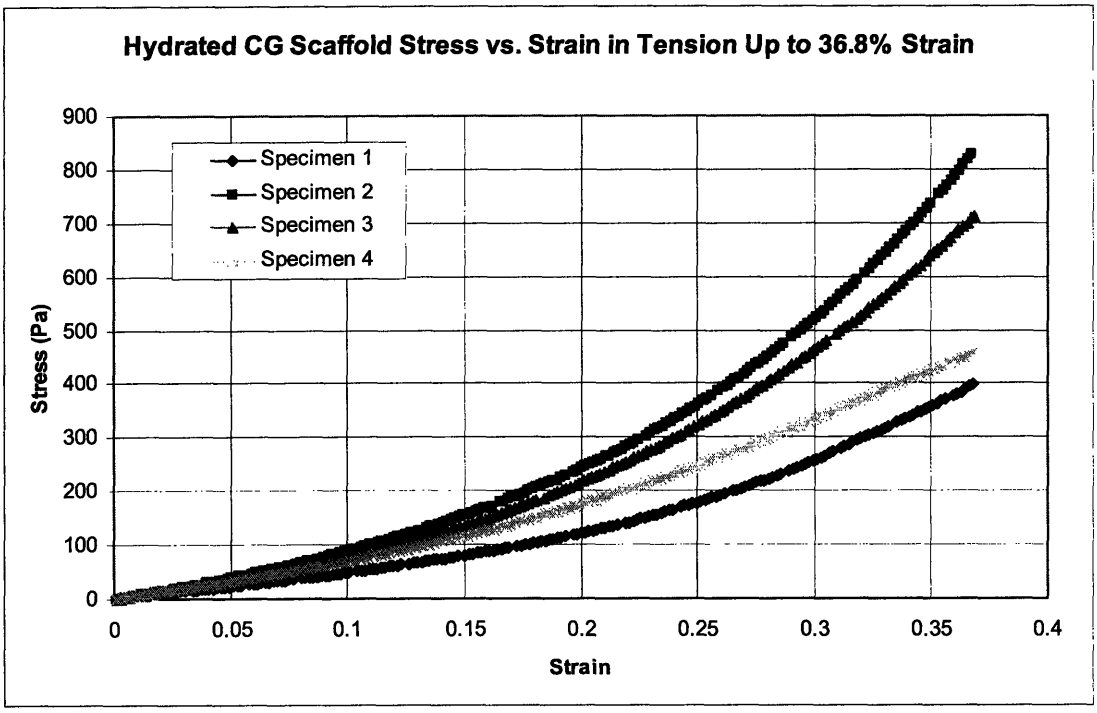

Figure 4.6: Stress vs. strain curve of hydrated collagen-GAG scaffolds

Although these curves exhibit a nonlinear stress-strain curve, there seemed to be a linear portion of the graph at low strains. Moreover, it was clear that the elastic modulus of hydrated collagen was much lower than that of dry collagen since the stresses required to stretch the specimens to up to 35% strain was under one thousand Pascals while dry specimens took stresses on the order of tens of thousands of Pascals to reach strains of just 15%.

The average of the stress-strain curves is shown in Figure 4.7, and the error bars indicate one standard deviation above and below the average.

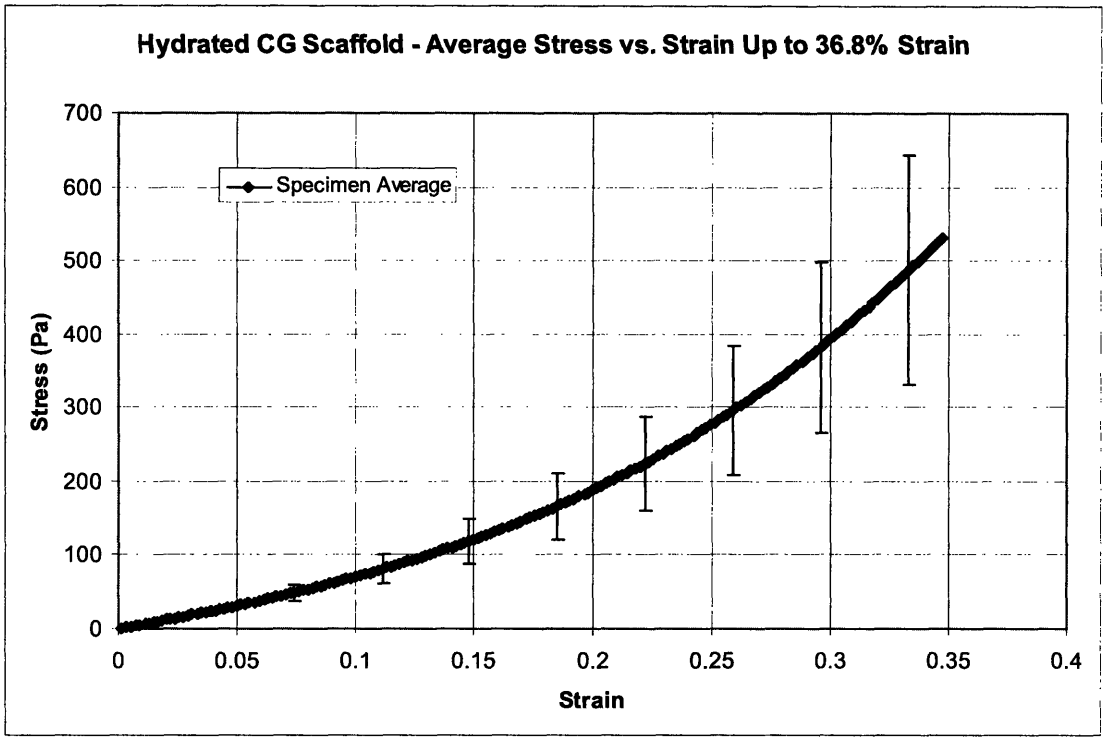

Figure 4.7: Average stress-strain curve of hydrated CG scaffolds Up to 36.8% Strain

Based on the apparently linear region at low strains, strains of 6, 9, and 12% were chosen as the strain levels at which to perform the stress relaxation curves. The hydrated stress vs. strain curve also exhibited much more variation in values especially at higher strains. The stresses that were associated with 6, 9, and 12% strain were found to be 38 ± 7.8 Pa, 62.5 ± 14.25 Pa, and 89.25 ± 21.9 Pa respectively.

Strains of up to about 35% were used in this data analysis because that was largest strain level common to all four specimens. Two of the specimens had also been tested all the way up to 60% strain, however, and the resulting stress-strain curves are shown in figure 4.8, where the error bars indicate one standard deviation above and below the average.

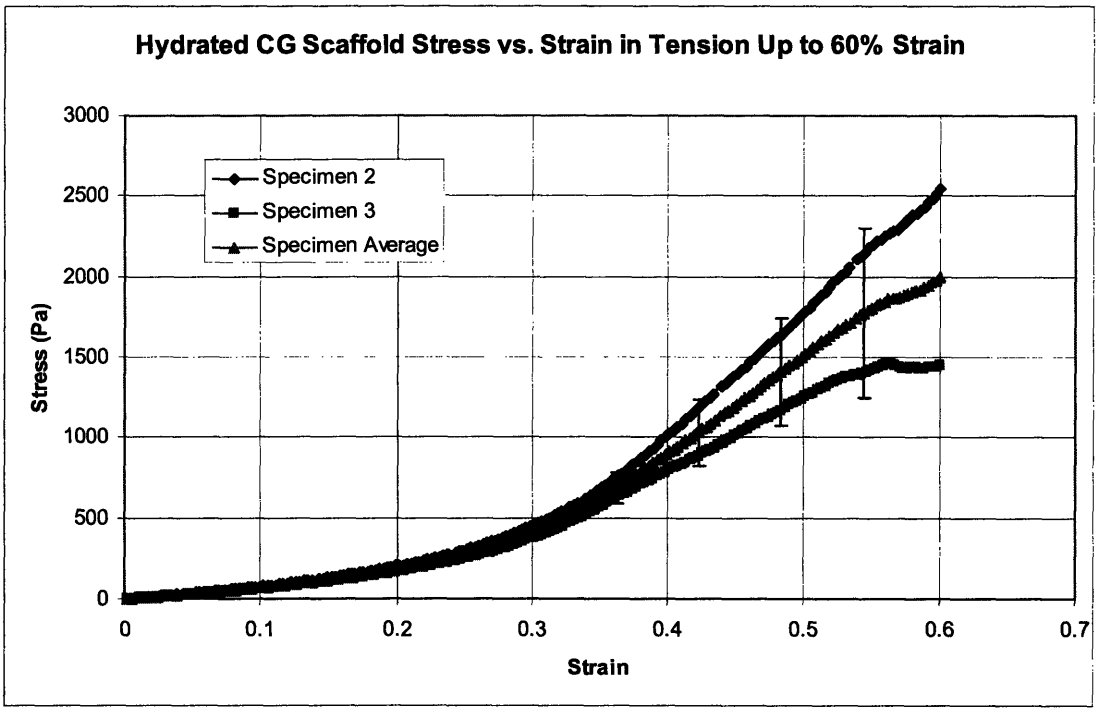

Figure 4.8: Stress vs. strain curves of hydrated CG scaffolds up to 60% strain

Although two samples is not enough to make a conclusive decision, it seems that based on this data in conjunction with the hyperelastic model, the linear region of the stress-strain curve begins after around 37 – 40% strain. Thus, as was done for the dry scaffolds, selecting strains in this linear region could also have been used for the stress relaxation tests.

4.4 Stress Relaxation Tests of Hydrated Collagen-GAG Scaffolds

Data analysis of the stress relaxation tests of hydrated collagen-GAG scaffolds proved to be very difficult for a variety of reasons. Many of the tests contained severe irregularities and either had to have sections removed from the middle of data sets or had to have the ends of the data sets truncated off. Moreover, many of the tests had varying initial stress levels and varying strain levels because they were run before realizing that tension tests would need to be performed to standardize the initial stress level. This made averaging the data extremely complicated and challenging. Ultimately, however, they should be able to give a general sense of the stress relaxation response of hydrated collagen-GAG scaffolds as well as an idea of whether or not there is linear viscoelastic behavior.

Figure 4.9 shows a graph of selected stress relaxation curves of hydrated collagen-GAG scaffolds at various strain levels. All tests were run for 5 hours, but some of the curves have been truncated because of disrupted results. The curves from top to bottom follow the order of the accompanying legend.

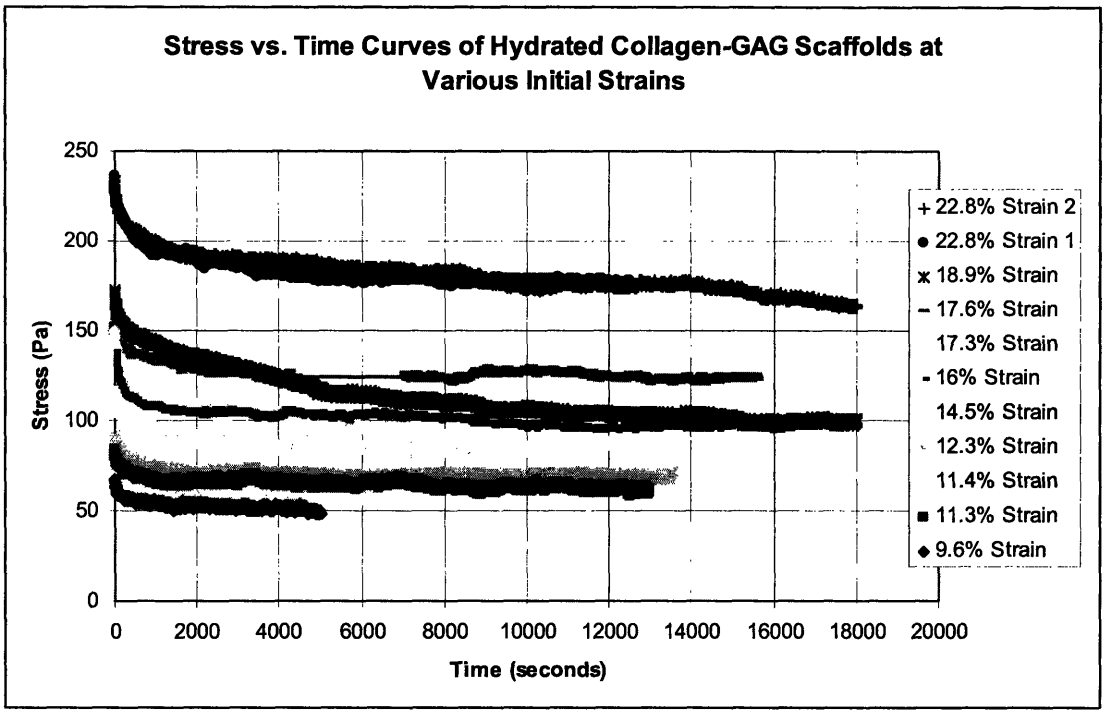

Figure 4.9: Stress relaxation curves of hydrated collagen-GAG scaffolds held at various strains levels

The strains for the curves in figure 4.9 were calculated retroactively in that the strains were obtained by comparing the peak stress level that the specimen achieved to the stress-strain curves obtained from the tension tests of the hydrated collagen-GAG scaffolds. Although it would have been nice to be able to standardize the strains ahead of time, it was unclear that it would be so difficult to accurately measure the initial gage length of the hydrated specimens. Most of these samples were supposed to have been loaded to 6% or 9% strains, but close to every single test was significantly above the target strain level.

In order to determine linear viscoelasticity, the relaxation modulus was once again calculated for each of the different curves by dividing the stress response by the corresponding strain. Because of the large number of stress relaxation curves, curves in similar strain regions were averaged together for comparison purposes. Curves with strains from 9.6% to 12.3% were grouped together, 14.5% to 18.9% were grouped together, and the 22.8% strain curves were grouped together. Figure 4.10 shows the relaxation modulus plotted against time for these three groups where the error bars indicate one standard deviation above and below the average.

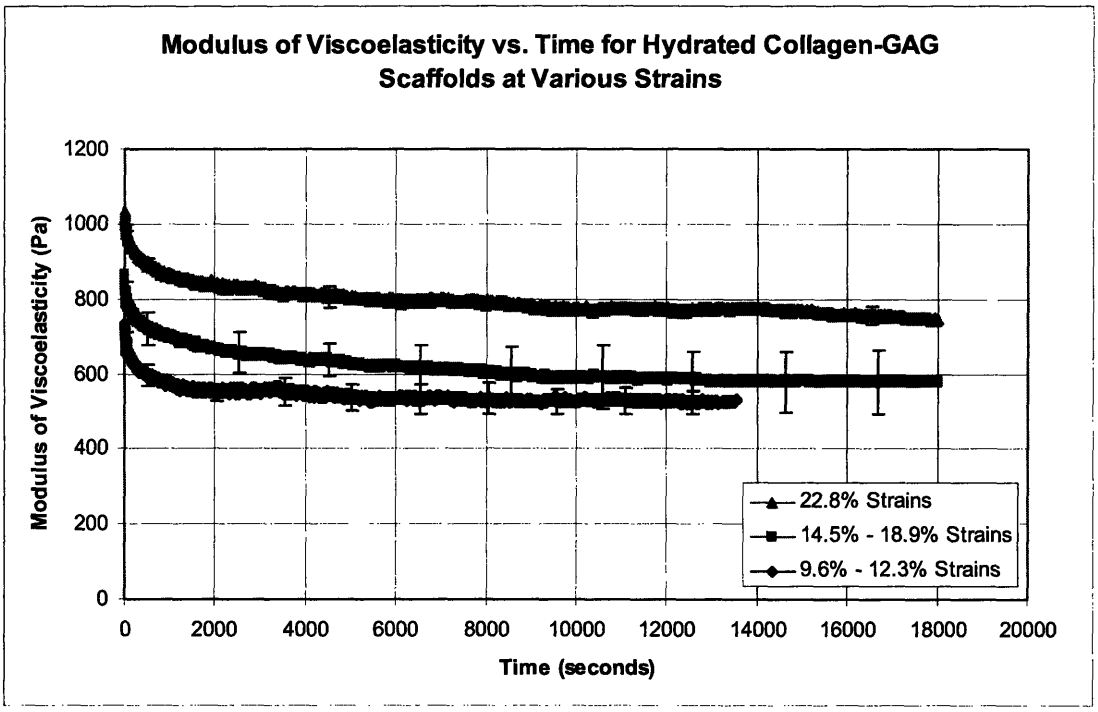

Figure 4.10: Relaxation modulus vs. time for hydrated collagen-GAG scaffolds at various strains

Similar to the dry collagen scaffolds, the hydrated collagen scaffolds also do not seem to demonstrate linear viscoelastic property since the modulus of viscoelasticity is not the same at different strain levels. The error bars for some of these curves do overlap, and consequently, there is less confidence of this result than for the results of the dry collagen-GAG scaffolds.

4.5 Water Bath

The water bath comprised the design component of this thesis, and as there is no mention of temperature during the tests, the water bath ended up not being used for the tests. It was decided that water bath design #2 (see section 3.4) would be pursued because of the difficulty of trying to directly control the temperature of such a small volume of liquid. Also, although the hydration chamber would not be directly heated, because of its small volume, it would not take a very high flow rate for the chamber to fill

with new water in a short period of time. The design #2 broke the water bath down into two obvious modules. The first module was the temperature control system including the water reservoir, the thermocouple, the heater, and temperature controller. The second module was the water circulation system that would pump water into and out of the hydration chamber from the water reservoir.

4.5.1 Temperature Control System

The first step in designing the temperature control system was actually to choose the size of the reservoir and then choose an appropriate heater for the volume and type of liquid, in this case 1x PBS solution, which can be compared to salt water. The larger the reservoir, the easier it would be to control the temperature since the flow of warm water to the hydration chamber and the flow of cooler water from the hydration chamber would affect the temperature of the reservoir less. However, there are space requirements since the lab bench is only so big, and the system also has to be relatively portable (i.e. not a permanent fixture). Based on available online water tanks, the best size was an 8" x 8" x 8" cube polyethylene tank with a volume of approximately 2 gallons; however, because of time and cost factors, ultimately, a 3 gallon tank with dimensions of approximately 6" x 12" x 18" was bought from Home Depot to be used as the reservoir.

Based on the 3 gallon tank size, the power requirements for the heater then needed to be calculated. The power needed was calculated by finding the initial power requirements, finding the operating power requirements, and then choosing the larger value (Omega Engineering 2006). The equation used to calculate the initial heating power requirements was:

$$\left(\frac{Qmc}{3412}+\frac{Ls}{2x1000}\right)x(\#\text{ heating hours}) \tag{4.2}$$

The first term of the equation refers to the amount of heat it takes to heat up the liquid and the container, where Q is energy, m is mass, and c is specific heat capacity. The second term in the equation is the heat loss to the exposed area over the time it takes to heat up the system, where L is the surface area, and s is the thermal conductivity of the material. The numerical factors arise because the equation is written to convert English units to metric. Based on specific heat capacity values obtained from Matweb, a volume of 3 gallons of water, and a warm up time of 30 minutes, the amount of initial heating power needed came out to be .120 kW. The equation used to calculate the operating heating requirement was simply:

$$\frac{Ls}{1000} \tag{4.3}$$

This came out to approximately .09 kW. Thus, the heater needed to have a power capacity of at least .120 kW. When selecting a heater, however, it was also necessary make sure that the heater didn't have too high of a power capacity. If the liquid being heated was too viscous and the heater's power was too large, there would be temperature gradients within the liquid that could disrupt the control system. Because of the very low

viscosity of water and because the power requirements were relatively low, however, a suitable over the side immersion heater with a power capacity of 1kW, and dispersion rate of 21 W/in^2.was chosen from the Omega website.

After having chosen the heater, the next step was to backtrack and choose a solid-state relay assembly that could handle carrying the necessary power to the heater as well as a compatible temperature controller. A standard dc input solid-state relay and dc output PID temperature controller were chosen for this purpose and met the power requirements needed by the heater. A finned heat sink also had to be bought for the solid-state relay to increase thermal cooling while the system was running. Additionally, a standard thermocouple with a 304 stainless steel sheath made from special limits of error material to ensure that the control system had the desired precision of .5 degrees Celsius. Thus, the temperature control module was completed.

4.5.2 Water Circulation Module

The next part of the design required determining how to circulate water from the water reservoir to the hydration chamber and back. The flow had to be significant enough that the hydration chamber would be maintained at the desired temperature, but it couldn't be so fast that it would disrupt the test. Moreover, the method of circulating the water needed to be determined, either by the use of pumps, capillary action, or a spill chamber.

The first step was determining the volume of the hydration chamber, which was found to be approximately 350 milliliters. Based on some simple calculations as to how quickly the temperature of the hydration chamber would drop, it was estimated that the water would need to flow through the chamber at a rate of at least 70 milliliters per minute, which would mean a turnover time of about 5 minutes. Ultimately, however, the rate of circulation in the chamber would be dictated by the rate at which water could be added without disturbing the tests.

Having estimated the desired flow rate, several different methods of circulation were examined. If the use of capillary action could be used, it would eliminate the need for at least one pump, which could reduce cost and might make the system less complicated. The design of the hydration chamber does not lend itself to this design, however, since the only access point is through the top of the chamber. The problem is that if the water level were to drop to a point below where the tube was inserted, it would be impossible for the circulation system to recover, and the chamber would simply dry out or overflow depending on whether capillary action was used for transporting water to or from the chamber. The unreliability and lack of robustness made it infeasible. Likewise the use of an spill ramp or overflow chamber would have similar problems in that there would be a huge mess in the event that unforeseen circumstances disrupted the intended flow of the circulation system. Hence, it was decided that two pumps would be needed to control the circulation of liquid: one to pump water from the reservoir to the hydration chamber and another to pump water form the hydration chamber to the reservoir.

Obtaining a pump for this purpose still proved to be a challenging endeavor. The main uses for liquid pumps outside of the laboratory are in fish tanks and aquariums; however, many of these pumps require submersion in liquid, have very high flow rates, and will break if allowed to run dry (i.e. if there isn't a continuous flow of liquid through it). Because of the size of the hydration chamber, the pumps needed to be external pumps since they wouldn't be able to fit inside the chamber. Also, we desired a slow flow rate in order to ensure that the tests would not be disrupted too much. Finally, because aquarium pumps cannot run dry, they need to be primed at the beginning of use, which means the tubes connecting them need to be filled completely with water, which is cumbersome and impractical for its use in this situation. Additionally, in the event that the water level dropped below the intake tube of a pump, the pump would overheat and breakdown, which was not a very robust and flexible design. Ultimately, some medium flow variable flow pumps from VWR (vwr.com), which have an adjustable flow rate of .5 to 85 milliliters per minute, do not require priming, and can run dry, were chosen.

4.5.3 Water Bath Implementation and Test Results

The final setup of the water bath is shown in figure 4.11. The temperature control system fit on the right side of the Zwick machine while the pumps and water circulation system were placed as close as possible to the hydration chamber itself.

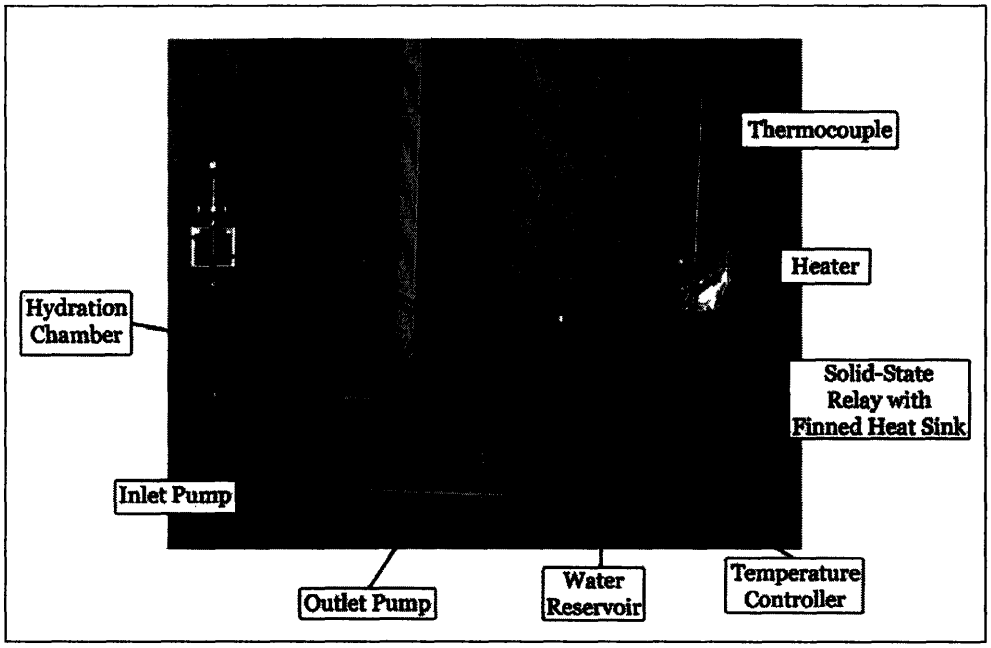

Figure 4.11: Set up of water bath with hydration chamber

At this point, the main concern of the project with regards to the water bath was whether or not the circulation of water into the hydration chamber would significantly disrupt the already very sensitive tests. The current caused by the water flowing through the pumps had to be insignificant and the water level had to be maintained at the same level throughout the process. In order to test this, the pumps were run without any specimens with a full hydration chamber. Both pumps were set to the same setting and

the machine was allowed to measure the force over time, which should remain constant or within .2mN, which is the resolution of the machine. Results from these tests are shown in figure 4.12.

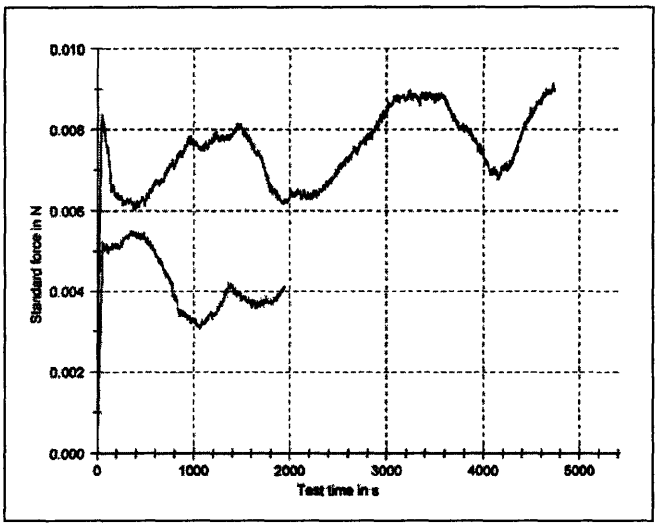

Figure 4.12: Force vs. time graph testing apparatus with water bath circulating into hydration chamber and no specimens loaded

Without any movement of the fixtures and without any specimens inside, the registered force on the testing machine fluctuated at least 2 millinewtons, which was too large of a fluctuation for the hydrated collagen-GAG scaffold tests. Ultimately the water bath would not be used in any mechanical testing because of the sensitivity of these tests. The water bath was originally intended to be used in a much less sensitive testing environment because it was not known that the elastic modulus of the hydrated collagen scaffolds would be quite this low. However, because of these unpredictable circumstances, although the design of the project was completed, the implementation failed because the functional parameters that had been originally laid out had changed beyond the scope of the flexibility of the designed system.

5. Conclusion

The purpose of these tests was to begin to develop a viscoelastic model for collagen-GAG scaffolds in order to study the response of these scaffolds to loading by cells over time in the body. Although the mathematical model to describe their behavior isn't yet made clear, the results of these experiments shown in figures 4.4 and 4.10.indicate that collagen-GAG scaffolds, whether hydrated or dry, do not exhibit linear viscoelastic properties. While the tests performed on dry specimens appeared to be relatively accurate, the unreliability and lack of standardization in the hydrated tests suggest that further testing would need to be done to create a more accurate mathematical model. Since much of the error seems to be caused by the low forces associated with the low strains in hydrated stress relaxation tests, performing tests at higher strain levels (see section 4.3) that fall in the linear elastic region would most likely give better results.

Another significant source of error is the measuring of hydrated specimens, especially the initial gage length. Because of the low modulus of elasticity of hydrated collagen, the specimens stretch easily when measured, which can cause varying amounts of pre-loading in specimens when perform relaxation tests. Combined with the sensitivity of the tests and the leaking of the hydration chamber, the results can be significantly skewed. Other mechanical tests to investigate the properties of hydrated scaffolds should be performed in a more controlled environment and a more standard method of measurement should also be developed. Lastly, the water bath designed would function well in a less sensitive testing environment. Depending on the forces required to achieve strains in the higher linear elastic region of the hydrated collagen-GAG scaffold stress-strain profiles, it might be useful in determining temperature dependence of viscoelastic properties in such tests. Otherwise, an altogether different method of controlling the temperature of the hydration chamber will need to be created since it would be almost impossible to create another bath of similar design that would disrupt the system less than the current design.

Nevertheless, these findings present several implications for future applications and research. The data on the viscoelastic profile of collagen-GAG scaffolds should be useful in investigating quantitatively how cells contract and apply force to the scaffold because the response of the scaffold to particular loads over time are now more clearly defined. Moreover, now that the time response has been characterized, it is possible to study the effect of particular viscoelastic properties on cell behavior in scaffolds such as cell migration, attachment, and contraction. Hopefully by continuing to develop the mathematical models that describe the mechanical behavior of these collagen-GAG scaffolds due to interactions with cells, a better understanding of a general theory of tissue regeneration through implantable scaffolds can be attained in order to achieve more successful regeneration in other tissues in the body as well.

6. References

1. Yannas, I.V. Tissue and Organ Regeneration in Adults, Springer-Verlag New York, LLC, 2001.

2. Yannas, I. V., Lee, E., Orgill, D. P., Skrabut, E. M., and Murphy G. F. (1989). Synthesis and characterization of a model extracellular matrix that induces partial regeneration of adult mammalian skin. Proc. Natl. Acad. Sci. USA 86, 933–937.

3. Roy, P., Petroll, W. M., Cavanagh, H.D., Chuong, C. J., and Jester, J. V. (1997). An in vitro Force Measurement Assay to Study the Early Mechanical Interaction between Corneal Fibroblasts and Collagen Matrix. Experimental Cell Research, 232, 106-117.

4. Freyman, T. M., Yannas, I. V., Yokoo, R., and Gibson, L. J. (2001). Fibroblast contraction of a collagen-GAG matrix. Biomaterials, 22, 2883 – 2891.

5. Freyman, T. M., Yannas, I. V., Pek, Y-S., Yokoo, R., and Gibson, L. J. (2001). Micromechanics of Fibroblast Contraction of a Collagen-GAG Matrix. Experimental Cell Research, 269, 140-153.

6. Troxel, K. (1994). Delay of skin wound contraction by porous collagen-GAG matrices, Thesis (Ph.D.), Massachusetts Institute of Technology, Dept. of Applied Biological Sciences.

7. Crandall, S. H., Dahl, N. C., et al., An Introduction to the Mechanics of Solids, McGraw-Hill Companies, Boston, Burr Ridge, IL, Dubuque, IA, Madison, WI, New York, San Francisco, St. Louis, 1999.

8. Bowman, S. M. (1997). Creep of Trabecular Bone, Thesis (Ph.D.), Harvard-MIT Division of Health Sciences and Technology & The Division of Engineering and Applied Sciences.

9. B.A. Harley, F.J. O'Brien, I.V. Yannas, L.J. Gibson (2004), "Fabrication and characterization of equiaxed collagen-GAG scaffolds," Trans. Soc. Biomat. 30.

10. Yannas, I. V. (1974). Nonlinear Viscoelasticity of Solid Polymers (in Uniaxial Tensile Loading). Macromolecular Review, 9, 163-190.

11. Grinnell, F. (1994). Fibroblasts, myofibroblasts, and wound contraction. J Cell Bio, 124, 401-404.

12. Desmouliere, A., Gabbiani, G.(1996). The role of the myofibroblast in wound healing and fibrocontractive diseases. In: Clark RAF, editor. The molecular and cellular biology of wound repair. New York: Plenum Press, 391-423.

13. Freyman, T. M., Yannas, I. V., Yokoo, R., and Gibson, L. J. (2002). Fibroblast Contractile Force Is Independent of the Stiffness Which Resists the Contraction. Experimental Cell Research, 272, 153-162.

14. Lo, C-M., Wang, H-B., Dembo, M., Wang, Y. (2000). Cell Movement Is Guided by the Rigidity of the Substrate. Biophysical Journal, 79, 144-152.

15. B.A. Harley, H.-D. Kim, M.H. Zaman, I.V. Yannas, L.J. Gibson, "Quantifying individual cell migration and contraction behavor in a series of well-characterized collagen-glycosaminoglycan scaffolds," Trans. World Congress on Tissue Engineering adn Regenerative Medicine, 2006.

16. B.A. Harley, L.J. Gibson, "Study of Cell-Mediated Contraction: Fabrication and Mechanical Characterization of Collagen-based Scaffolds," Proceedings of the 23rd Scientific Conference of the Society for Physical Regulation in Biology and Medicine, 2005.

17. Ashby, M. F., Jones, D. R. H., Engineering Materials I, Butterworth-Heinemann, Jordan Hill, Oxford, Woburn, MA, 1996.

18. Bischoff, J.E., Arruda, E.M., Grosh, K. (1999). Finite element modeling of human skin using an isotropic nonlinear elastic constitutive model. Journal of Biomechanics 33, 645-652.

19. O'Brien, F. J., Harley, B.A., Yannas, I.V., and Gibson L.J. (2003). Influence of freezing rate on pore structure in freeze-dried collagen-GAG scaffolds, Biomaterials, 25, 1077-1086.

20. http://www.matweb.com/search/SpecificMaterial.asp?bassnum=O4000

21. Pek, Y.S., Spector, M., Yannas, I.V., Gibson, L.J. (2003). Degradation of a collagen-chondroitin-6-sulfate matrix by collagenase and by chondroitinase, Biomaterials, 25, 473-482.

22. Chamberlain, L., Yannas, I., Hsu, H., and Spector, M. (2001). Connective tissue response to tubular implants for peripheral nerve regeneration: The role of myofibroblasts. *J. Comp. Neurol.* 417, 415-430.

23. Omega Engineering, Omega Complete Electric Heaters Handbook and Encyclopedia, Omega Engineering Inc., Stamford, CT, 2001.